NATIONAL AERONAUTICS AND SPACE ADMINISTRATION

Space Programs Summary No. 37-33, Volume VI

for the period March 1, 1965 to April 30, 1965

Space Exploration Programs and Space Sciences

jpl
JET PROPULSION LABORATORY
CALIFORNIA INSTITUTE OF TECHNOLOGY
PASADENA, CALIFORNIA

May 31, 1965

NATIONAL AERONAUTICS AND SPACE ADMINISTRATION

Space Programs Summary No. 37-33, Volume VI

for the period March 1, 1965 to April 30, 1965

Space Exploration Programs and Space Sciences

JET PROPULSION LABORATORY
CALIFORNIA INSTITUTE OF TECHNOLOGY
PASADENA, CALIFORNIA

May 31, 1965

Preface

The *Space Programs Summary* is a six-volume, bimonthly publication that documents the current project activities and supporting research and advanced development efforts conducted or managed by JPL for the NASA space exploration programs. The titles of all volumes of the *Space Programs Summary* are:

Vol. I. The Lunar Program (Confidential)

Vol. II. The Planetary–Interplanetary Program (Confidential)

Vol. III. The Deep Space Network (Unclassified)

Vol. IV. Supporting Research and Advanced Development (Unclassified)

Vol. V. Supporting Research and Advanced Development (Confidential)

Vol. VI. Space Exploration Programs and Space Sciences (Unclassified)

The *Space Programs Summary,* Vol. VI consists of an unclassified digest of appropriate material from Vols. I, II, and III; an original presentation of technical supporting activities, including engineering development of environmental-test facilities, and quality assurance and reliability; and a reprint of the space science instrumentation studies of Vols. I and II. This instrumentation work is conducted by the JPL Space Sciences Division and also by individuals of various colleges, universities, and other organizations. All such projects are supported by the Laboratory and are concerned with the development of instruments for use in the NASA space flight programs.

W. H. Pickering, *Director*
Jet Propulsion Laboratory

Space Programs Summary No. 37-33, Volume VI

Prepared under Contract No. NAS 7-100, National Aeronautics & Space Administration

Contents

LUNAR PROGRAM

PLANETARY–INTERPLANETARY PROGRAM

DEEP SPACE NETWORK

SUPPORTING ACTIVITIES

SPACE SCIENCES

LUNAR PROGRAM

I. *Ranger* Project

A. Introduction

The *Ranger* Project was established to develop a space flight technology for transporting engineering and scientific instruments to the Moon and planets. Nine *Ranger* launchings, using *Atlas D–Agena B* vehicles, were planned; all of these flights have now been made.

Rangers I and *II* (Block I) were not lunar-oriented, but were engineering evaluation flights to test the basic systems to be employed in later lunar and planetary missions. Several scientific experiments were carried on a non-interference basis. Both spacecraft performed satisfactorily within the constraints of the obtained satellite orbit. *Rangers III, IV,* and *V* (Block II) carried a gamma-ray instrument, a TV camera, and a rough-landing seismometer capsule; each of these flights experienced failures.

The objective of the *Ranger* Block III (*Rangers VI, VII, VIII,* and *IX*) flights was to obtain pictures of the lunar surface, at least an order of magnitude better than those obtainable with Earth-based photography, which will be of benefit to both the scientific program and the U.S. manned lunar flight program. The *Ranger VI* spacecraft, which was launched from the Air Force Eastern Test Range (AFETR) on January 30, 1964, and impacted the Moon essentially on target on February 2, 1964, did not accomplish the primary flight objective due to a failure of the TV subsystem to transmit pictures. An extensive analysis of the TV subsystem failure was conducted, new and reworked hardware was assembled as the *Ranger VII* TV subsystem, and extensive testing of the reassembled TV subsystem was performed.

The *Ranger VII* spacecraft was launched from the AFETR on July 28, 1964, and impacted the Moon on target on July 31, 1964. The mission flight objective was accomplished. The outstanding events of the mission were the precision of the trajectory correction and the transmission of 4304 video pictures of the lunar surface.

The *Ranger VIII* spacecraft was launched from the AFETR on February 17, 1965, and impacted the Moon on target on February 20, 1965. The mission flight objective was again accomplished, and approximately 7000 high-quality video pictures of the lunar surface were transmitted from the spacecraft. The final calculated impact point represented a miss of only 15 miles from the originally selected aiming point.

The *Ranger IX* spacecraft was launched from the AFETR on March 21, 1965, and impacted the Moon on target on March 24, 1965. Again, the mission flight objective was accomplished; following a successful terminal maneuver, 5814 excellent-quality video pictures of the lunar surface were transmitted from the spacecraft. The resolution of the final pictures is the best resolution obtained during any of the Block III flights. For the first time, the video signals, as relayed from the Goldstone

Space Communications Station to JPL by microwave link, were scan-converted for live commercial TV transmission. The final calculated impact point of *Ranger IX* represented a miss of only 4 miles from the originally selected aiming point.

B. TV Subsystem Performance

1. Ranger VIII

The performance of the *Ranger VIII* TV subsystem from its prelaunch checkout to its operation in the terminal phase of the mission was as predicted. Critical events for the mission are given in Table 1.

A prelaunch reduced-power test conducted on the TV subsystem showed the camera and telemetry performance to be as expected, indicating a state of launch readiness. During the launch phase, the Spacecraft Data Monitoring Station was able to maintain lock with the spacecraft until the *Atlas–Agena* went over the horizon. The data indicated that the TV subsystem performance was normal throughout this critical boost phase.

At spacecraft–*Agena* separation, the TV backup clock (programmed to begin Channel F warmup at S + 64 hr, 15 min) was initiated, as shown by a change from 0 to 0.8 v on Point 9 of the cruise-mode telemetry. At S + 30 min, the spacecraft hydraulic timer commanded *ground-enable* for the silicon-controlled-rectifier turn-on circuits. These circuits are disabled during the boost phase to ensure that subsystem operation is not inadvertently initiated in the critical pressure region of the atmosphere. At L + 61 min, a backup *ground-enable* command was provided by a microswitch actuated by the deployment of the $-x$ solar panel and monitored by a data encoder B2-4 event.

As the spacecraft turned to acquire the Sun at L + 63 min, the Camera F_a lens was turned into the Sun momentarily, causing the sharp temperature rise noted in Fig. 1(a). After completion of Sun acquisition, the temperature returned to nominal. At L + 3 hr, 30 min, the top hat (Fig. 1b) increased in temperature. This increase resulted from the turning of the spacecraft during the Earth-acquisition phase of the flight. After completion of Earth acquisition, the top hat temperature returned to nominal.

Table 1. Critical events of the *Ranger VIII* mission

Event	Time of event[a]	
	Predicted[b]	Actual, GMT[c]
Prelaunch reduced-power test	L − 115 min	048:13:59
Start of cruise-mode telemetry	L − 15 min	048:16:40
Launch	L	048:17:05:00.795
Separation	S	048:17:30:14
TV *ground-enable* command by hydraulic timer	S + 30 min	048:18:00:14
Backup TV *ground-enable* command by microswitch on $-x$ solar panel	L + 61 min, S + 46 min	048:18:05:39.5
8-hr Clock pulse	S + 8 hr	049:01:30:12
16-hr Clock pulse	S + 16 hr	049:09:30:35
TV Channel 8 removed from bus carrier for this interval	Telemode II; end of pitch turn to M + 30 min	049:10:21:30 to 049:10:30:38.6
24-hr Clock pulse	S + 24 hr	049:17:30:48
32-hr Clock pulse	S + 32 hr	050:01:30:52
48-hr Clock pulse	S + 48 hr	050:17:31:08
64-hr Clock pulse	S + 64 hr	051:09:31:29
Warmup of Channels F and P by central computer and sequencer	I − 24 min, 20 sec	051:09:33:10
Full power of Channels F and P by internal sequencer	I − 23 min, 6 sec	051:09:34:30
Clock backup of warmup on Channel F	S + 64 hr, 15 min	051:09:46:29[d]
Central computer and sequencer backup of full-power command	I − 19 min, 20 sec	051:09:38:10
Impact	I	051:09:57:36.8

[a]The clock events have a tolerance of +0, −15 sec due to the commutation of the telemetry data.
[b]Launch (L), separation (S), midcourse (M), and impact (I).
[c]Day of year:hr:min:sec.
[d]Estimated.

At S + 8 hr and S + 16 hr, confirmation was received that the clock was functioning properly.

In the cruise mode, the TV subsystem furnished 15 commutated points of battery, backup clock, and temperature measurements. During the midcourse maneuver, this telemetry was switched off from the end of the pitch turn to the start of Sun reacquisition to allow motor-burn information to be transmitted over Channel 8. Also, due to problems in the bus transmitter area, Channel 8 was lost from the stop of the roll turn to the start of motor burn. During the maneuver, the temperatures in the TV subsystem fluctuated. The top hat (Fig. 1b) and the

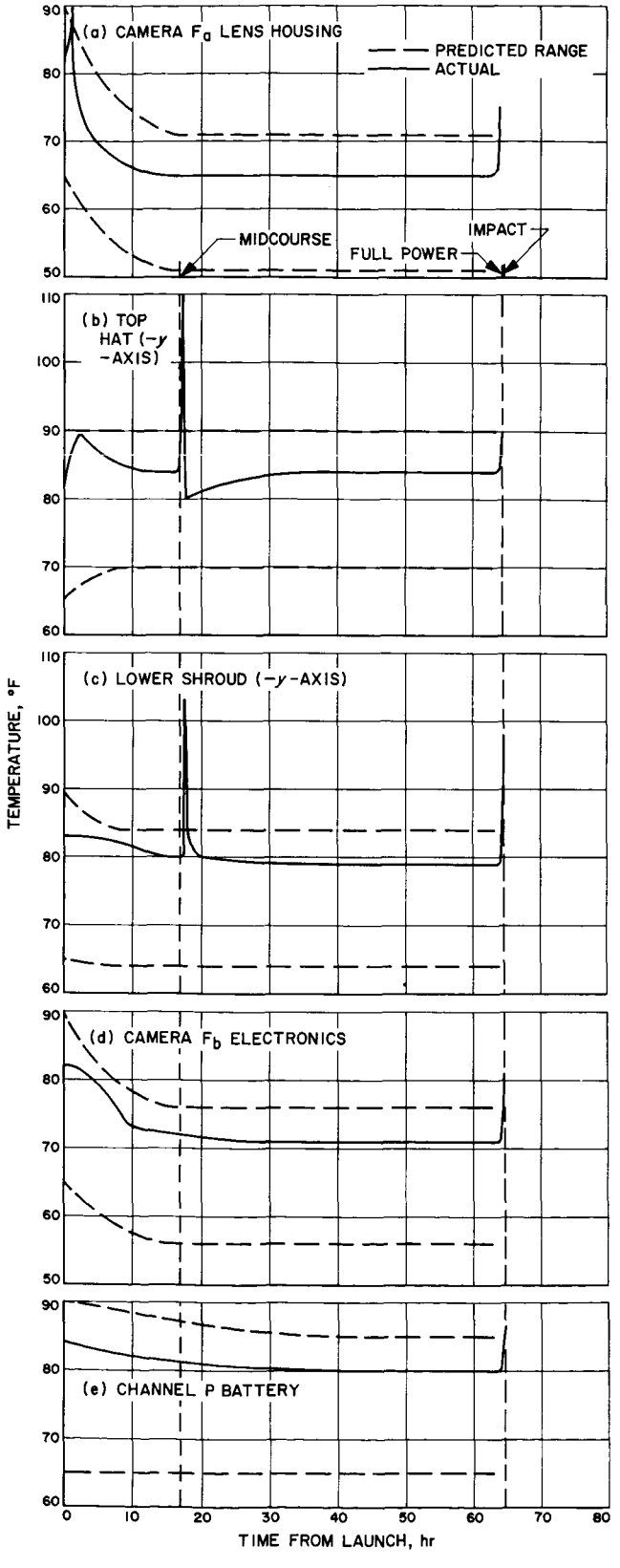

Fig. 1. Actual and predicted temperatures of the *Ranger VIII* spacecraft from launch until impact

lower shroud (Fig. 1c) exhibited sharp rises in temperature during the pitch turn and the Sun-reacquisition phases of the midcourse maneuver. After about 15 hr, the temperatures stabilized.

Without a midcourse maneuver, the clock would have turned Channel F into warmup at I − 2 hr, 8 min. With the midcourse correction used, the scheduled time of clock turn-on of Channel F was I − 11 min. The nominal corrected time of I − 30 min was not chosen for the time of TV initiation by the clock due to the cone angle constraints on the omni-antenna.

During the remainder of the cruise period, confirmations of proper clock operation were received at S + 24, 32, 48, and 64 hr. All current voltages and temperatures indicated that the TV subsystem was functioning normally. By trading off higher resolution on the final pictures for over-all broader coverage and possible stereoscopic effects, it was decided to leave the spacecraft in its cruise-oriented position. Therefore, in the terminal maneuver, RTC-8 (Real-Time Command 8) was sent prior to RTC-6 in order to disconnect the spacecraft attitude-control subsystem from the central computer and sequencer (CC&S). This enabled the use of timing functions of the CC&S without changing the spacecraft attitude.

In order to obtain a larger area of coverage for the initial pictures, RTC-6 was sent at I − 69 min, 26 sec. The TV-2 command was generated 45 min after the spacecraft receipt of RTC-6. It, in turn, indicated warmup in both Channels F and P at approximately I − 24 min, 26 sec. This event was monitored by noting the change from 15- to 90-point telemetry and was confirmed by noting a change in Points 55 and 60 from 0 to 2.4 v and a change in current level from approximately 0 to 8 amp on Channel F and from 0 to 10 amp on Channel P. The rest of the data received during this warmup period indicated normal operation for both channels. The current drain, battery voltage, and heat-sink temperatures indicated that both channels would be able to operate for the required 24 min, 26 sec. Since the CC&S performed flawlessly, the need to initiate an RTC-7 (which had been held in readiness) never arose. During this terminal period, the temperature on the Camera F_a lens housing (Fig. 1a) increased 10°F due to reflected and radiated light energy from the lunar surface.

The battery voltages, which had plateaued at −34.8 v for Channel F and −34.7 v for Channel P, fell to −32.4 v for Channel F and −32.3 v for Channel P when high current demands were placed on the batteries during the

terminal phase of the mission. These voltage levels indicated that the batteries were operating under normal load and, with the predicted usage data, further indicated that the batteries had at least another 30 min of life remaining in them at the end of the mission.

Both channels turned into full-power operation by means of the internal 80-sec sequencer. This was confirmed by a change in Points 55 and 60 from 2.4 to 0.6 v and a change in current on Channel F from 8 to 13 amp and on Channel P from 10 to 15 amp. At this point, the Goldstone Space Communications Station confirmed the receipt of strong video from both Channels F and P. However, because of the initial high light level, the F_a, P3, and P4 pictures exhibited minimum detail in the early frames.

The backup clock initiated a warmup command to Channel F. Since both channels were previously turned on by the CC&S, the clock command had no effect, and its turn-on time could only be estimated. The estimate was that the clock was 1 min slow for the entire 64-hr, 15-min period; this performance was well within the design tolerance of ± 5 min.

The CC&S backup command (TV-3) to initiate full power on both channels was timed to occur 50 min after the spacecraft received RTC-6. This event was noted by monitoring a blip on the B2-1 channel of the data encoder. Again, since both channels were previously turned into full power by the TV subsystem's internal 80-sec sequencer, the TV-3 command had no effect.

The temperature of the top hat (Fig. 1b), lower shroud (Fig. 1c), and Camera F_b electronics (Fig. 1d) increased sharply at the end of the mission due to the heat generated by the TV subsystem in full-power operation. The Channel P battery temperature increase (Fig. 1e) resulted from the high current drain during the terminal portion of the mission. The transmitter heat sink temperatures exhibited their expected rise. The readings were sufficiently below the maximum temperatures to permit operation of the TV subsystem for at least another 19 min. One peculiarity noted throughout the flight was that the temperatures of the TV subsystem were about 5°F higher than the predicted nominal. However, these temperatures were still well within the over-all stabilized limits.

It was anticipated and noted that the Channel 8 voltage-controlled oscillator exhibited a minor slow drift of 1 or 2 cps over the entire mission. This is within the over-all tolerance of ± 5 cps for the unit.

The TV subsystem performance during the 64 hr, 52 min, 36 sec of the *Ranger VIII* mission was as predicted. All operating parameters were within design specification, and all cameras and systems performed perfectly, except for microphonics on Camera P2. These microphonics were observed during ground testing of *Ranger VIII*, but at about 1-order-of-magnitude lower frequency than that during the mission. The reasons for this increase in microphonics can never be fully ascertained, but the increased temperature caused by the 24 min, 26 sec of operation was felt to be one of the major contributors.

The 6597 P-camera pictures and the 538 F-camera pictures gave a broad coverage of the lunar surface, viewing both the highland areas and the by-now-familiar mares. In order to obtain this broad coverage, resolution on the final pictures was sacrificed due to increased smear.

2. Ranger IX

The performance of the *Ranger IX* TV subsystem from its prelaunch checkout to its operation in the terminal phase of the mission was as predicted. Critical events for the mission are given in Table 2.

As with *Ranger VIII*, the prelaunch testing and launch operations were normal. At *Agena*–spacecraft separation, the TV backup clock (programmed to begin Channel F warmup at S + 63 hr, 30 min) was initiated. At S + 30 min, the spacecraft hydraulic timer commanded *ground-enable* for the silicon-controlled-rectifier turn-on circuits. At L + 61 min, a backup *ground-enable* command was provided by a microswitch actuated by the deployment of the $-x$ solar panel and monitored by a data encoder B2-4 event.

As the spacecraft passed through the Earth's shadow for approximately 34 min during the early phases of the mission, the temperatures throughout the TV subsystem dropped; this is especially evident in the temperatures of the top hat (Fig. 2b), the lower shroud (Fig. 2c), and the Camera F_b electronics (Fig. 2d). A few hours after the spacecraft passed out of the Earth's shadow, the temperatures stabilized at their nominal levels.

Telemetry confirmation of proper clock operation was received at S + 8, 16, 24, and 32 hr. The telemetry indicated the clock was averaging 10 sec slow for each 8-hr period. This time was within the specification for accumulated clock counting.

Table 2. Critical events of the *Ranger IX* mission

Event	Time of event[a]	
	Predicted[b]	Actual, GMT[c]
Prelaunch reduced-power test	L − 115 min	080:17:55
Start of cruise-mode telemetry	L − 15 min	080:20:41
Launch	L	080:21:37:02
Loss of Channel 8 telemetry	L +	080:21:44:42
Separation	S	080:21:52:26
TV *ground-enable* command by hydraulic timer	S + 30 min	080:22:22:26
Backup TV *ground-enable* command by microswitch on −x solar panel	L + 61 min, S + 46 min	080:22:37:51
8-hr Clock pulse	S + 8 hr	081:05:52:36
16-hr Clock pulse	S + 16 hr	081:13:52:47
24-hr Clock pulse	S + 24 hr	081:21:52:54
32-hr Clock pulse	S + 32 hr	082:05:53:01
TV Channel 8 removed from bus carrier for this interval	Telemode II; end of pitch turn to M + 30 min	082:12:22:56 to 082:12:33:38
48-hr Clock pulse	S + 48 hr	082:21:53:26
Backup clock disabled	I − 50 min, 40 sec	083:13:17:38
Warmup of Channels F and P by central computer and sequencer	I − 20 min, 20 sec	083:13:48:13
Full power of Channels F and P by internal timer	I − 19 min	083:13:49:33
Central computer and sequencer backup of full-power command	I − 15 min, 20 sec	083:13:53:13
Impact	I	083:14:08:20

[a]The clock events have a tolerance of +0, −15 sec due to the commutation of the telemetry data.
[b]Launch (L), separation (S), midcourse (M), and impact (I).
[c]Day of year:hr:min:sec.

As with *Ranger VIII*, during the midcourse maneuver, the telemetry information was switched off from the end of the pitch turn to the start of Sun reacquisition to allow motor-burn information to be transmitted over Channel 8. During the maneuver, the spacecraft turned 128 deg in the pitch direction. This increased the solar heat input to the −y side of the TV tower, causing the top hat temperature (Fig. 2b) to increase 45°F and the lower shroud temperature (Fig. 2c) to increase 21°F. When the spacecraft turned to reacquire the Sun, the temperatures returned to nominal.

During this phase of the *Ranger IX* mission, trajectory studies indicated that the clock would turn Channel F into warmup at I − 1 hr, 3 min. With the midcourse

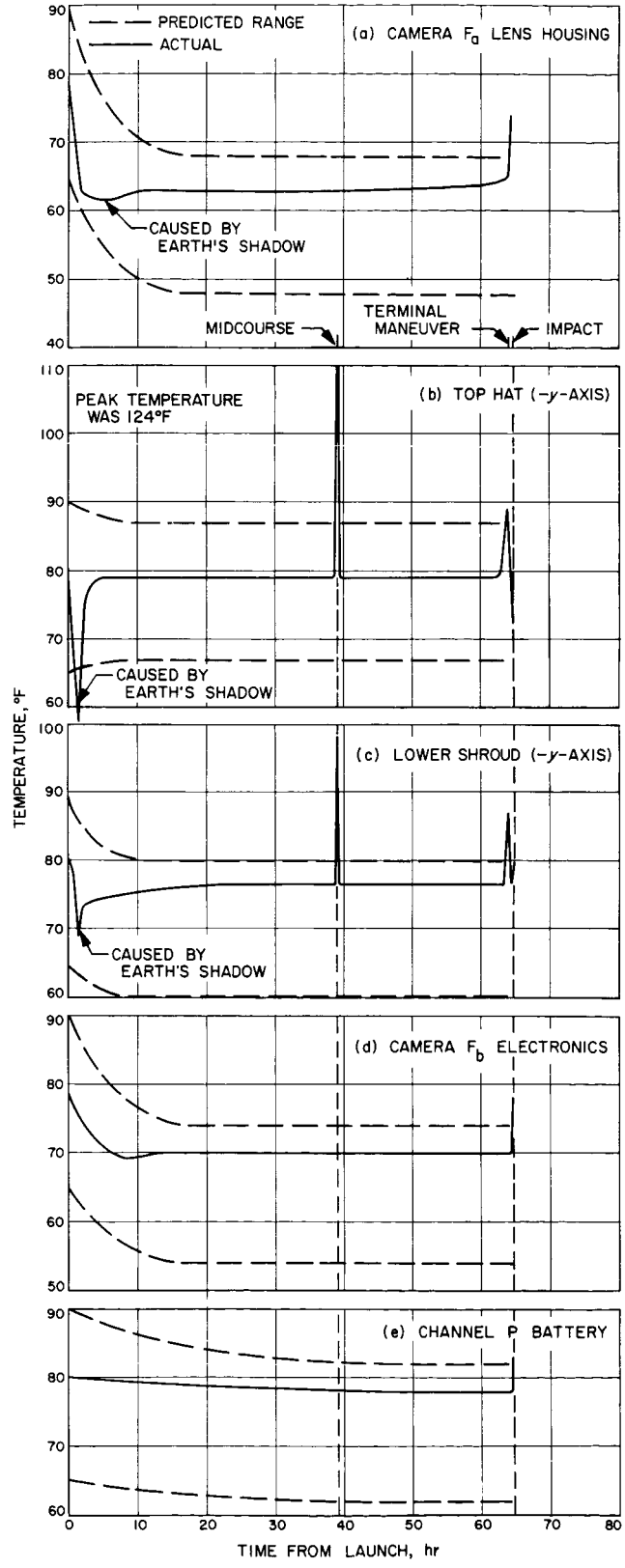

Fig. 2. Actual and predicted temperatures of the *Ranger IX* spacecraft from launch until impact

correction selected, the scheduled time of the clock turn-on of Channel F was $I - 45$ min. The nominal corrected time of $I - 30$ min was not chosen for the time of TV initiation by the clock due to the cone angle constraints on the omni-antenna as well as post-midcourse dispersion-ellipse constraints. Another factor in reducing the post-midcourse dispersion ellipse was the initiation of midcourse at $L + 39$ hr instead of the nominal $L + 16$ hr, thereby having more precise trajectory inputs on which to base the maneuver. By following this approach, the built-in protection against disabling the clock by RTC-5 was eliminated since the inhibit on clock turn-off is released at S + 32 hr.

During the remainder of the cruise period, continued confirmation of proper clock operation was received at S + 48 hr. All current voltages and temperatures indicated that the TV subsystem was functioning normally throughout the cruise period.

In order to have the TV pictures nest over the crater Alphonsus and to reduce smear to a minimum level, it was decided to accomplish a terminal maneuver. To obtain a larger area of coverage for the initial pictures, the RTC-6 was to be sent at $I - 65$ min, initiating TV warmup at $I - 20$ min. The exact time of the RTC-6 (83:13:03:13 GMT) was so adjusted that the last picture of the F-cameras would be an F_b, with three times the magnification of the F_a's which were the last pictures on *Rangers VII* and *VIII*.

The first pitch turn of the terminal maneuver was 5 deg. This caused the $-y$ side of the TV tower to be turned slightly into the Sun, causing the top hat temperature (Fig. 2b) and lower shroud temperature (Fig. 2c) to rise 10°F.

Due to the trade-off constraints imposed upon the midcourse correction and subsequent trajectory correction, the Channel F backup clock would have initiated Channel F operation at approximately $I - 45$ min. As the command link was functional, and since the terminal maneuver had initiated and verified that the CC&S counter was functional, it was decided to disable the clock by sending an RTC-5. The pictures obtained at $I - 45$ min would have less resolution than existing lunar photographs and would possibly impose thermal limitations upon the TV subsystem. Telemetry indicated that the clock reset since the clock telemetry indication (Point 15-9) returned to zero. The Channel F current decreased to 0 amp, and the Channel F battery voltage increased approximately 0.5 v.

The second pitch turn of the terminal maneuver was -20 deg, causing the $-y$ side to be placed in shadow and thus causing the temperatures on the top hat and the lower shroud to fall.

At 45 min after the initiation of RTC-6, the CC&S counter, by means of a TV-2 command, turned both channels into warmup at $I - 20$ min, 7 sec. This event was monitored by noting the change from 15- to 90-point telemetry and was confirmed by noting a change in Points 55 and 60 from 0 to 2.4 v and a change in current level from approximately 0 to 8 amp on Channel F and from 0 to 10 amp on Channel P. The rest of the data received during this warmup period indicated normal operation for both channels. The current drain, battery voltage, and heat sink temperature indicated that both channels would be able to operate for the required 20 min, 7 sec. Since the CC&S performed flawlessly, the need to initiate an RTC-7 (which had been held in readiness) never arose. During the terminal period, the temperature on the Camera F_a lens housing (Fig. 2a) increased 10°F due to reflected and radiated light energy from the lunar surface and was apparently the same as that for *Ranger VIII*.

As in *Ranger VIII*, the battery voltages plateaued at -34.8 v for Channel F and -34.7 v for Channel P. The battery voltages dropped to -32.5 v when the high current demands were placed on the batteries during the terminal phase of the mission. These voltage levels indicated that the batteries were operating under normal load and, with the predicted usage data, further indicated that the batteries had at least another 30 min of life remaining in them at the end of the mission.

Both channels turned into full-power operation by means of the internal 80-sec sequencer. This was confirmed by a change in Points 55 and 60 from 2.4 to 0.6 v and a change in current on Channel F from 8 to 13 amp and on Channel P from 10 to 15 amp. At this point, the Goldstone Space Communications Station confirmed the receipt of strong video from both Channels F and P. By having a terminal maneuver, the pictures nested very well, and all cameras recorded high-quality video photographs.

The CC&S backup command (TV-3) to initiate full power on both channels was timed to occur 50 min after the spacecraft received RTC-6. This event was noted by monitoring a blip on the B2-1 channel of the data encoder. Since both channels were previously turned into full power by the TV subsystem's internal 80-sec sequencer, the TV-3 command had no effect.

The heat generated by the full-power operation of the TV subsystem caused the drop in temperature on the top hat (Fig. 2b) to be limited to 6°F below the nominal. On the lower shroud (Fig. 2c), the added heat caused the temperature trend to reverse, raising the shroud temperature to 80°F. On the Camera F_b electronics (Fig. 2d), the added heat caused the temperature to rise sharply to 88°F. The Channel P battery temperature increase (Fig. 2e) resulted from the high current drain during the terminal portion of the mission. The transmitter heat sink temperatures exhibited their expected rise. However, the starting temperatures of the Channel F and P transmitters differed by 8°F. This was caused by uneven heating due to the terminal maneuver's net effect of a change in spacecraft orientation to −15 deg off the Sun-oriented position. This led to a final temperature that was 10°F higher than that originally predicted for Channel F. One peculiarity noted throughout the mission was that the temperatures of the TV subsystem were about 5 to 8°F higher than the predicted nominal. However, these temperatures were still well within their over-all stabilized limits.

The TV subsystem performance during the 64 hr, 31 min, 18 sec of the *Ranger IX* mission was as predicted. All operating parameters were within design specification, and all cameras and systems performed perfectly.

The 5814 pictures gave a nested view of the crater Alphonsus, with good contrast and high shadowing on the final pictures. The resolution of the final F_b, P1, and P3 pictures was 0.3 m—the best resolution obtained during any of the *Ranger* Block III missions.

C. Space Flight Operations

1. Ranger VIII

On February 17, 1965, the *Ranger* Space Flight Operations (SFO) System supported the countdown for the *Ranger VIII* mission. Liftoff occurred at 17:05:00.795 GMT[1], with all systems operating satisfactorily. The solar panels opened normally at 60 min after launch (18:05), with the spacecraft going into a Sun acquisition mode at 18:09. The Spacecraft Data Analysis Team (SDAT) reported that the spacecraft was operating on solar-panel power at 18:12, that the antenna had reached the preset hinge angle at 18:14, that Earth acquisition had begun at 20:36, and that the spacecraft had acquired a body later confirmed as the Earth at approximately 20:40. A command sequence was initiated from the Johannesburg Tracking Station, culminating in an RTC-3 (Real-Time Command 3; antenna switchover) being transmitted at 21:25. The SDAT confirmed the transfer from the omni-antenna to the high-gain antenna at 21:29. The flight proceeded normally from that time until midcourse, with the exception that the communications circuits to the Johannesburg Tracking Station were quite often marginal.

The midcourse sequence was initiated from the Goldstone Echo Station at 10:00 on February 18 with the transmission of an RTC-4 to the spacecraft. A positive roll turn of 53 sec, with all indications normal, was verified by the SDAT. Upon completion of the roll turn, the received signal strength at the Goldstone Echo Station began to vary radically from −142 dbm to threshold, causing all telemetry channels to go in and out of lock. Sufficient information was derived from the sporadic telemetry by the SDAT to lead the SFO Director to believe that the spacecraft was performing normally and that only the telecommunications link to Earth was at fault. Upon start of motor burn, the signal strength increased to its normal value, all telemetry channels were in lock, and all indications were normal. The motor-burn duration was 59 sec as commanded. Doppler plots indicated that the velocity vector was in the correct direction. The SDAT had reported that the spacecraft was back on full solar-panel power by 10:37, that the high-gain antenna had gone to the preset angle at approximately 10:38, that Earth reacquisition had begun at 10:59, and that Earth reacquisition was complete at 11:03. A command sequence was initiated from the Goldstone Echo Station to transmit RTC-3 to the spacecraft at 11:34. At 11:36, the SDAT verified that the transfer from the omni-antenna to the high-gain antenna was complete. The spacecraft was thereby returned to its normal cruise mode until the initiation of the terminal-maneuver sequence.

As on the *Ranger VII* mission, it was determined that the terminal-maneuver counter would be enabled; however, it would not control the attitude of the spacecraft. Therefore, limited-duration (1-sec) turn commands were sent to the spacecraft. Prior to the initiation of the terminal maneuver, an RTC-8 was sent at 08:27 on February 20. This command, in effect, disconnected the attitude-control subsystem from the central computer and sequencer. The terminal-maneuver initiation command, RTC-6, was transmitted from the Goldstone Echo Station at 08:47:30

[1]All times given here are GMT.

on February 20. The SDAT indicated all spacecraft parameters were normal with no indication of turns. Channels F and P of the TV subsystem both went into warmup at 09:33, with a report of both channels in full power occurring at 09:34. The quality of the pictures obtained was reported as excellent. Impact occurred at 09:57:37.

2. *Ranger IX*

The *Ranger IX* launch countdown was initiated at 12:51 on March 21, with an available launch window of 63 min starting at 21:11. The *Ranger IX* SFO System was reported to be in a "go" condition beginning at 16:21. This condition continued throughout the countdown, but with some difficulties occurring in communications with the Johannesburg Tracking Station caused by poor propagation conditions. The countdown proceeded normally toward a scheduled liftoff time of 21:11. At approximately $T-2$ min, 50 sec, a hold was called for the *Agena*. The countdown was recycled and held at the $T-7$ min point. The count was resumed at 21:30, with liftoff occurring at 21:37:02.456 on a launch azimuth of 93.7 deg. At 22:38, the Deep Space Instrumentation Facility (DSIF) reported a series of B-2 events indicating that the solar panels were open. The SDAT reported that the spacecraft was in a Sun acquisition mode and that the high-gain antenna was deploying at 22:41, that the spacecraft was on solar-panel power by 22:46, and that Sun acquisition was complete at 22:48.

At 01:09 on March 22, the SDAT reported that the Earth sensor was on and dark and that the spacecraft was in an Earth acquisition search, and, at 01:12, that Earth acquisition was complete. The DSIF reported at that time that the Johannesburg Tracking Station was experiencing noise spikes on the output of its transmitter. Therefore, it was decided to delay the transmission of an RTC-3 to the spacecraft until the Goldstone Echo Station view period. At 09:30, command procedures were instituted from the Goldstone Echo Station to transmit an RTC-3 to the spacecraft. The SDAT confirmed completion of the transfer of telecommunications from the omni-antenna to the high-gain antenna at 09:33. This placed the spacecraft in its normal cruise configuration.

Tracking data received from both the AFETR and the DSIF indicated an extremely accurate injection, with a flight path which would have resulted in an impact only 323 miles north of the primary aiming point of the crater Alphonsus. At that time, it was determined that the midcourse maneuver could be performed on either the first (launch + 17 hr) or second (launch + 39 hr) Goldstone pass with little difference in the dispersions at the aiming point due to midcourse execution errors. Additional multistation tracking data available for a second Goldstone pass maneuver would yield a significant decrease in the orbit uncertainty with no degradation in the final results. This, then, led to the choice of the second Goldstone pass maneuver.

A second pass maneuver was selected which adjusted the flight time such that the backup clock would turn on the Channel F TV cameras 45 min prior to impact. The SDAT reported that the preset antenna hinge angle was predicated on a 17-hr maneuver, and not a 39-hr maneuver, and requested that an additional RTC-2 be sent to the spacecraft to update the preset hinge angle for the later maneuver. A command procedure was initiated at the Woomera Tracking Station at 22:30, resulting in an RTC-2 (antenna hinge-angle update command) being sent to the spacecraft. The SDAT observed a B-20 event which occurred at 22:30:39.

Starting at 10:54 on March 23, the Goldstone Echo Station initiated the transmission of the three stored commands for the midcourse maneuver to the spacecraft. These commands consisted of a roll turn of -27 deg, a pitch turn of 128 deg, and a motor-burn duration of 30 sec. By 11:05, the Goldstone Echo Station had verified the telemetered content of the stored commands as being correct. At 11:35, this station initiated an RTC-3 to transfer the telecommunications from the high-gain antenna to the omni-antenna for the duration of the maneuver. The SDAT confirmed that the telecommunications had been transferred successfully to the low-gain antenna at 11:37.

As instructed by the SFO Director, the Goldstone Echo Station transmitted an RTC-4 to the spacecraft at 12:03:00 to initiate the midcourse-maneuver sequence. Normal execution of turns and motor burn by the spacecraft was confirmed by the SDAT. The midcourse maneuver was completed by 12:33, at which time the spacecraft went into a Sun reacquisition mode. By 12:49, the SDAT had confirmed that the spacecraft was on solar-panel power only and, by 12:52, that Sun acquisition was complete. At 13:01, Earth reacquisition was initiated by the spacecraft. The SDAT confirmed that Earth reacquisition was complete at 13:04. The Goldstone Echo Station initiated an RTC-3 at 13:30, transferring the telecommunications from the omni-antenna back to the high-gain antenna.

The SDAT reported that antenna switchover was satisfactorily completed at 13:33 and that the spacecraft was back in normal cruise configuration at that time.

Impact geometry was such that a terminal maneuver was required to place the reference axis of the camera system along the velocity vector of the spacecraft. The terminal-maneuver sequence was initiated from the Goldstone Echo Station with the transmission of an SC-4 (Stored Command 4) at 11:58 on March 24. This command was followed at 2-min intervals by an SC-5 and an SC-6. The SC-4 directed a 24-sec pitch turn, the SC-5 directed a −75-sec yaw turn, and the SC-6 directed a −94-sec pitch turn. The Goldstone Echo Station verified the telemetered content of the stored commands from the spacecraft at 12:06 and initiated the terminal-maneuver sequence with the transmission of RTC-6 at 13:03. The SDAT verified the first pitch turn as being correct at 13:04 and the yaw turn as being correct 10 min later. The SFO Director then instructed the Goldstone Echo Station to transmit an RTC-5 at 13:17, thereby inhibiting the TV backup clock. The SDAT verified the end of the second pitch turn and its accuracy at 13:32.

At 13:48, the SDAT verified that both the F- and P-camera chains were in warmup, and, at 13:49:20, both channels of the TV subsystem went to full power. Goldstone reported excellent video on both channels at 13:50 and all camera operations normal. The Goldstone transmitter failed at 14:00, thereby losing the up-link to the spacecraft. No attempt was made to reacquire up-link lock in accordance with contingency planning detailed in the SFO Plan. Impact occurred at 14:08:20 with the impact point approximately 12.91-deg south latitude and 2.38-deg west longitude, just northeast of the central peak in the crater Alphonsus.

D. Guidance and Control

1. Ranger IX Power Subsystem Performance

As in the *Ranger VI, VII,* and *VIII* missions, the power subsystem performance during the *Ranger IX* mission was normal in all respects. The flight performance agreed quite well with preflight predictions, and no failures or degradations were noted.

a. Batteries. Both batteries operated normally throughout the flight. As with *Rangers VI, VII,* and *VIII,* only a small percentage of the available capacity was utilized: approximately 15.5%. This amount of usage did not provide sufficient data to determine the actual maximum-capacity capability.

b. Solar panels. The solar panels operated within their predicted limits during the entire flight.

Shroud ejection at 21:42:13 GMT was indicated by an increase in solar-panel voltages resulting from the exposure to ambient space illumination. The amount of incident energy on the panels was enough to provide a change in the telemetry transducer, but was insufficient to provide any significant power to the spacecraft.

During the cruise portions of the mission, the panel temperatures were 128°F, which is about 8°F higher than the *Ranger VII* panel temperatures. This is a result of the difference in solar intensity during the flight periods. At the time of the *Ranger VII* mission (July 1964), the solar intensity was 135 mw/cm^2. During the *Ranger VIII* and *IX* flights, the solar intensity was 142 mw/cm^2.

The telemetry data showed a slight unbalance in the solar-panel currents (0.2 amp), which agrees with the preflight test measurements performed on each panel.

During the pitch turn of the midcourse maneuver, an increase in the $+x$ solar panel voltage occurred at a time when the panel was not being illuminated by the Sun. An investigation revealed that the panel was receiving energy from the Moon. At the time of the maneuver, the Sun–probe–Moon angle was approximately 115 deg. One data point on the $+x$ panel showed an increase in panel voltage at a pitch angle of approximately 118 deg. The reason that a similar change in voltage was not detected on the $-x$ panel is that the Moon–probe clock angle was approximately 27 deg and the $-x$ panel was shaded by the spacecraft.

As a result of the terminal maneuver performed by *Ranger IX,* a detectable increase in panel temperatures did not occur. As predicted, the terminal maneuver resulted in a partial shading of the $+x$ panel from the end of the yaw turn until impact. The change in panel power capability was very small compared to the available power.

2. Block III Attitude-Control Subsystem Performance

a. Introduction. The functions of the Block III attitude-control subsystem, which remained the same throughout the *Ranger VI* through *IX* missions, were as follows:

(1) To acquire and maintain three-axis orientation with respect to the Sun and Earth.

(2) To point the high-gain communications antenna at the Earth.

(3) To orient the thrust vector of the midcourse motor in a predetermined direction in space and to maintain the orientation during the motor-burn period.

(4) To provide a measure of the spacecraft velocity during the motor-burn period for control of the midcourse velocity vector magnitude.

(5) To orient the spacecraft so that the TV camera optical axis was pointed in a predetermined direction and, at the same time, continue to point the high-gain antenna at the Earth during the terminal maneuver phase.

Two configurations of the attitude-control subsystem were used for these missions. The first configuration, for *Rangers VI* and *VII*, utilized position error signals from Sun sensors and rate signals from three single-degree-of-freedom gyros. These signals, through a switching amplifier, resulted in controlling torques being applied to the spacecraft by a nitrogen gas expulsion system. In the second configuration, for *Rangers VIII* and *IX*, once the Earth had been acquired and the position and rate error signals had been reduced to within their limit-cycle values, the rate signals from the gyros were switched out and replaced with derived-rate feedback signals. The capability of the subsystem to go to derived-rate control did not affect the acquisition, commanded turn, or midcourse autopilot performance; however, the cruise performance was considerably different, primarily due to the reduced limit-cycle rate increment and the lack of gyro noise.

The attitude-control subsystem configuration change was made in order to enhance the over-all reliability of the spacecraft. With the subsystem in the derived-rate mode of operation, a failure in the gyros, the gyro three-phase inverter, or the power synchronizer would not disable the attitude control.

b. Block III performance summary. During prelaunch operations, the proper antenna preset angle was selected by ground command. This angle was predetermined and was chosen to supplement the Earth–spacecraft–Sun angle at Earth acquisition. Since the orientation of the spacecraft axes at the launch complex was known, the outputs of the three gyros could be correlated to the known Earth rate. In general, correlation of the gyro data was within 1 deg/hr of the Earth rate.

The spacecraft separation rates were all within the 48-mrad/sec specification limit. Some of the rates did exceed the 9-mrad/sec limit of the telemetry measurement.

In response to the Sun acquire command, power was applied to the attitude-control subsystem. Upon this initial application of power, the subsystem was in a configuration such that the switching amplifier was receiving position error signals from the primary and secondary Sun sensors (pitch and yaw) and rate signals from all three gyros. The spacecraft rates were increased or decreased to the acquisition rates until the pitch and yaw rate and position errors were reduced to the limit-cycle values. The roll rates were at this time reduced to within their limits.

At approximately 2.5 hr after Sun acquisition, the power to the Earth sensor was switched from the Earth sensor heater to the Earth sensor power supply. At this point, the roll position error had been replaced by a roll search generator, causing the spacecraft to search in a negative direction. When a body of sufficient brightness entered the Earth sensor field-of-view, the search generator was switched out and the roll and hinge error signals were switched in. The roll position and roll rate error signals were then reduced to limit-cycle values. The *Ranger VIII* and *IX* derived-rate subsystem had a slower acquisition rate than the *Ranger VI* and *VII* subsystem; also, the derived-rate subsystem transferred to a derived-rate mode of operation after Earth acquisition.

The performance of the subsystem in the cruise configuration was basically that of limit-cycle operation. The deadbands of the limit cycle were within the nominal ± 2.8 mrad in pitch and yaw and a variable scale in roll (variable as the spacecraft-to-Earth distance increased and the angular diameter of the Earth decreased). Of the external torques on the spacecraft, only the torques in pitch appeared to be significant. These were caused by the high-gain antenna presenting an unsymmetrical area to the solar radiation about the pitch axis.

The velocity increment of the spacecrafts during the cruise phase was nominal. The velocity-increment design goal of the derived-rate subsystem was considerably lower than that of the *Ranger VI* and *VII* configuration.

During the midcourse maneuver, the position sensors were switched out, and the gyros provided rate and position signals to the subsystem. Of significance was the low acceleration constant in roll during the *Ranger VI* and *VII* missions. This low acceleration constant was found to have been caused by an error in the assumed roll moment-of-inertia. Between the *Ranger VII* and *Ranger VIII* missions, the roll moment-of-inertia was remeasured, and a new gas jet nozzle design was incorporated.

The Sun and Earth reacquisitions were identical to the initial acquisitions. The terminal maneuver configuration was similar to the midcourse configuration, except that Earth lock was maintained. In general, the performance of the *Ranger VI, VII, VIII,* and *IX* attitude-control subsystems was nominal during the missions. To date, no anomalies have been detected in analyses of the flight data.

II. *Surveyor* Project

A. Introduction

The *Surveyor* Project will be the next step in developing lunar technology. It will attempt soft landings on the Moon with a group of test missions whose objective is to demonstrate successful soft landing by post-landing spacecraft operation. An engineering payload including elements of redundancy, increased diagnostic telemetry, touchdown instrumentation, and survey TV will be used.

Following the test missions, the general objective is to conduct lunar exploration to extend our knowledge of the nature of the Moon and to discover and verify the suitability of sites for *Apollo* spacecraft landings. These flights will carry a scientific payload consisting of the following experiments: two-camera TV, micrometeorite ejecta, single-axis seismometer, alpha-particle scattering, soil properties (surface sampler), and touchdown dynamics.

The spacecraft will be injected into the lunar trajectory using *Atlas–Centaur* vehicles. A 50-m/sec midcourse correction capability will exist.

Surveyor Mission A is scheduled for launch during the latter part of 1965. The primary objective for this flight will be to demonstrate successful operation of the launch vehicle, spacecraft, space flight operations, Deep Space Instrumentation Facility, and ground communications from launch through the completion of the midcourse maneuver. The secondary objective will be the successful operation of the spacecraft from the midcourse maneuver through landing. The tertiary objective will be to accomplish spacecraft functions after landing.

Hughes Aircraft Company (HAC) is under contract to develop and manufacture the first seven flight spacecraft.

B. Systems Testing

1. SC-1 Flight Spacecraft

The initial systems checkout portion of the SC-1 flight-acceptance test was completed at HAC. The only significant spacecraft problem involved the interface between the TV subsystem and the spacecraft transmitters. The video was degraded by saturation of the transmitters. New transmitters with the pre-emphasis stage removed were incorporated to eliminate this problem. A

system confidence check and a mission sequence using batteries for power were then completed prior to the start of the upgrading period for SC-1. To allow sufficient time for upgrade of the TV cameras, they were removed before the start of the mission sequence. The environmental phases of the flight-acceptance tests will begin after upgrading operations have been completed.

2. SC-2 Flight Spacecraft

Group tests were completed at HAC on the RF mechanisms auxiliary, the command decoding and signal processing subsystem, and the radar altimeter and doppler velocity sensor (RADVS) subsystem utilizing spacecraft power. Only minor problems involving the system-test-equipment-assembly–spacecraft interface were encountered, and these were subsequently resolved. The first upgrade period for the SC-2 spacecraft units and spaceframe was then begun. After upgrading operations have been completed, the system will undergo initial system checkout.

3. T-21 Prototype System-Test Spacecraft

During the first two phases of solar-thermal-vacuum testing of the T-21 vehicle at HAC, a flight-control malfunction and a RADVS klystron power supply modulator malfunction occurred, causing the test sequences to be discontinued. However, the data obtained during the second phase substantiated the fact that the majority of the spacecraft systems (electronic, mechanical, and thermal) were functioning properly. Prior to the start of the third phase of testing, the faulty units were repaired, and the spacecraft batteries were replaced.

The third phase of testing consisted of three 20-hr abbreviated mission sequences under nominal, high, and low solar intensities, preceded by a standard pumpdown sequence and followed by a shutdown sequence. Although spacecraft malfunctions did occur, the test was considered successful from a functional and thermal standpoint.

In the T-21 type-approval vibration test phase, the entire z-axis portion, including spacecraft functional checkout, was completed. The most significant functional difficulty concerned a high level of microphonics on the receiver.

4. SD-1 Dynamic-Test Flight Model

SD-1 vehicle launch operations were conducted at the Air Force Eastern Test Range, and all prelaunch functions were normal. The *Atlas–Centaur 5* launch on March 2, 1965, failed when the booster engines of the *Atlas* vehicle shut down immediately after liftoff, causing the launch vehicle to fall back onto the pad and explode.

The S-band transponder was destroyed by the explosion and resulting fire; however, the transponder continued to operate for about 12 min after liftoff. During this time, both the RF system-test equipment assembly located in the Explosive Safe Facility and the listening post in Building AO reported receiving the signal. The lockup in transponder mode was performed by the operator of the RF system-test equipment assembly as verification that the signal was received. At approximately 9 min after liftoff, the transponder was observed to switch to the high-power mode, as reported by both receiving stations. The operation continued on high power until the signal failed completely.

During the attempt to launch *Atlas–Centaur 5*, the *Surveyor* transmitter was observed to go into the high-power mode at approximately $T + 550$ sec. Based on the immediate postlaunch investigation, it is felt that the following is the most likely explanation for this occurrence: Excessive heat from the fire could have resulted in the transfer high-power command line being shorted to spacecraft battery voltage in the spacecraft wiring harness, thereby initiating a transfer to high power. Similarly, this condition could have occurred in the *Centaur* wiring harness since all evidence indicates that the spacecraft remained attached to the *Centaur* forward section.

5. SD-2 Dynamic-Test Flight Model

The SD-2 vehicle has been undergoing tests at General Dynamics/Convair. Flight-acceptance vibration tests were completed with no major failure occurring. After flight-acceptance testing, the pre-interim combined system-test inspection, cleanup, calibration, and system testing were performed. As of March 12, the spacecraft was ready for the interim combined system test.

C. Space Flight Operations

In the *Surveyor* Project, there are two major areas of operational support mission-dependent equipment: (1) the command and data handling system consisting of the command and data handling console (CDHC) and its

associated test equipment, and (2) the spacecraft TV ground data handling system.

1. Command and Data Handling System

HAC was assigned the task of designing, building, and manning three CDHCs: one each for the Goldstone Pioneer Tracking Station, the Johannesburg Tracking Station, and the Tidbinbilla Tracking Station. The CDHC was originally designed to operate in conjunction with the Deep Space Instrumentation Facility (DSIF) to provide the capability to accurately generate and transmit commands to the spacecraft and to receive, demodulate, record, and display telemetered data from the spacecraft. At that time, there was no Space Flight Operations (SFO) Facility at JPL nor on-site data processing subsystem at the DSIF stations, and, therefore, no requirement for transmitting data to other ground stations. A requirement was later placed on the CDHCs to transfer spacecraft telemetered data to the on-site data processing computers, which, in turn, would monitor and edit the data and transmit them to the SFO Facility at JPL. The CDHCs were also required to receive messages from the SFO Facility by means of the on-site data processing computers to perform command tape generation, verification, and search.

The prototype CDHC was installed at the Goldstone Pioneer Station for engineering tests in early-1964. In December, certain parts were returned to HAC for modifications. The new and modified CDHCs were shipped to the three tracking stations in early-1965.

The CDHC at the Goldstone Tracking Station is presently undergoing engineering and compatibility tests with the station. In April, it was connected to the on-site data processing subsystem for the first time. After minor problems were resolved, the CDHC successfully communicated with the on-site data processing computers on all input and output lines. The CDHCs at the Johannesburg and Tidbinbilla Tracking Stations are presently undergoing installation and engineering tests.

2. Spacecraft TV Ground Data Handling System

This system is being implemented for installation at the SFO Facility at JPL and the Goldstone Pioneer Station facilities to support *Surveyor* missions that include TV experiments. The system will: (1) record all spacecraft TV data with the highest reasonable quality and ensure the continued availability of the recordings, (2) provide outputs and real-time displays for support of SFO of *Surveyor* missions in real time, and (3) provide off-line non-real-time support in the form of photographic records. At the Goldstone Pioneer Station, three types of recordings will be obtained: predetection recordings of spacecraft TV data, FM recordings of demodulated spacecraft TV data, and 70-mm film recordings of the data. The spacecraft TV data will be relayed to the SFO Facility for recording by the microwave link from the Goldstone Pioneer Station. All of the recording capability of the system at the Goldstone Pioneer Station is duplicated in the SFO Facility at JPL.

The preliminary configuration of the system was installed in the SFO Facility in September 1964. It consisted basically of a scan converter system and an associated data recovery subsystem. This configuration was used to provide real-time display of the *Ranger IX* spacecraft TV images.

Film recording capability will be incorporated at the Goldstone Pioneer Station in July 1965, and the complete system is expected to be operational in September.

D. Telecommunications

1. Touchdown Dynamics Experiment Real-Time Telemetry Link

The proposed touchdown dynamics experiment for the A-21A (scientific payload) series spacecraft includes the real-time transmission of six gyro and accelerometer signals. A telecommunications study was conducted to determine the feasibility of obtaining these data at the desired time. Two areas were investigated: (1) the telemetry link limitations in terms of available signal bandwidth and output signal-to-noise ratios, and (2) the factors that affect the probability of obtaining the data. Factors that could affect the real-time telemetry link are: (1) antenna dynamics at touchdown, (2) transmitter frequency deviation due to shock at touchdown, (3) antenna gain available at touchdown, and (4) lunar reflection of omnidirectional antenna energy.

It was concluded that it is feasible to provide a telecommunications system capable of transmitting six real-time channels during touchdown. It was also determined that the most serious problem could result from the reflection of RF energy from the lunar surface, and it was recommended that this be investigated in more detail.

E. Flight Control

Investigation is in progress to determine the effect of moonlight on Canopus sensor performance as the spacecraft approaches the Moon before the pre-retrorocket maneuver. Test results show that moonlight interference will have no effect on Canopus sensor performance for the first launch; however, when all possible lunar landing latitudes for later launch dates are considered, there are some landing latitudes that may present interference. Canopus sensor performance under these situations is being evaluated by further tests.

With the addition of the acquisition Sun sensor to the top of the flight-control sensor group, further testing for possible Canopus sensor interference due to reflected sunlight from nearby structures was initiated. Tests to determine Canopus sensor effects due to acquisition Sun sensor and landing leg reflections are also under way.

Flight-acceptance tests were completed on three acquisition Sun sensors. Two are being integrated into sensor group wiring harnesses in preparation for the assembly of the flight-control sensor groups, and the third has successfully completed type-approval tests.

F. Propulsion

1. Vernier Propulsion Subsystem

During a detailed study of all the contributors to a spacecraft center-of-gravity shift during flight, it was concluded that spacecraft moment control is inadequate during main retro firing. As a result, it was decided to remove the propellant manifolds of the vernier propulsion subsystem, thereby eliminating the possibility of propellant migration. The S-6 vehicle (vernier-propulsion system-test spacecraft) has been modified to include this design change, and a series of checkout firings have been conducted. The data are currently being analyzed.

2. Seismometer Release Device

In conjunction with the development of the seismometer assembly to be soft-landed on the Moon during the *Surveyor* science mission (*SPS 37-20*, Vol. VI, pp. 90–93, and *SPS 37-27*, Vol. VI, pp. 45–48), a concurrent development of a release device was initiated. The release was required to uncage the central moving magnet of the seismometer, which, to prevent damage to the instrument during periods of high acceleration, was fixed firmly to the seismometer housing. For flexibility and ease of installation, a steel cable of 0.093-in.-D was chosen to hold the magnet to the housing. Releasing or severing the cable on command in the lunar environment was the problem to be solved.

The spatial constraints and energy requirements to release the cable, which was to be tensioned up to 600 lb, appeared to make the problem solution best suited to a pyrotechnic device. Since no suitable developed hardware was available, the device was to be developed at JPL.

The concept of releasing the cable rather than cutting it provided a feasible solution for redundant action within a small space. The configuration selected was a pinpuller design. The complete unit is shown in Fig. 1.

Unusually severe test conditions were imposed on the first fabricated units to observe design weaknesses quickly, and all units functioned satisfactorily. At the completion of approximately 16 firings (8 units), 60 units were obtained for type-approval testing. This program was composed of design verification tests, severe in nature, and sequential environmental tests, all expected

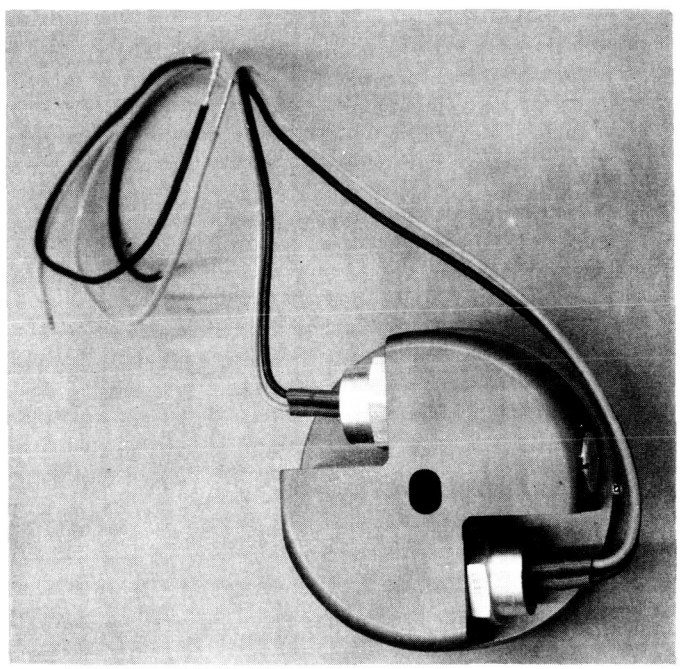

Fig. 1. Seismometer release device

to be considerably more degrading than the flight environments. Presently, the design verification portion has been successfully completed, and the units are being exposed to the sequential environments. Functioning of several devices is being provided at the end of each exposure to check the effect of the individual environment.

G. Testing Facilities and Equipment

1. Material Outgassing Test Chamber

A test chamber to determine the outgassing characteristics of materials under the lunar environmental conditions similar to those anticipated for the *Surveyor* spacecraft is shown in Fig. 2. The material sample under test is supported at one end of the chamber and can be held to any specific temperature in hard vacuum. The optical surface on which the outgassed products may condense is located at the opposite end of the chamber and can also be temperature-controlled. Circular baffles welded to the chamber walls surround the path between the sample location and the optical condensing surface.

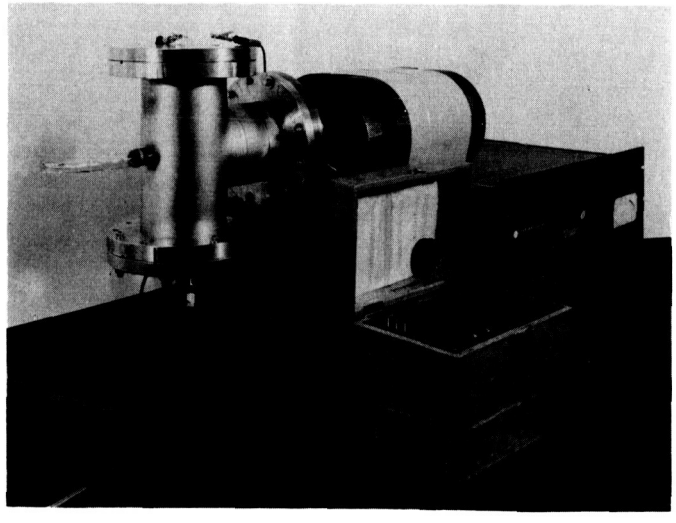

Fig. 2. Material outgassing test chamber

Liquid nitrogen is circulated through the double walls and baffles of the chamber.

The products of outgassing condense if they strike the cold walls of the chamber or the baffles. The products that condense on the optical surface are those which travel only in the direct path. In this way, close simulation of the conditions on the spacecraft in the lunar or free-space environments can be established and studied.

2. Data Acquisition Center

As a result of recent developments, a command and data handling console is no longer available for the interim version of the data acquisition center. However, the *Mariner C* (*Mariner* Mars 1964) computer data system at JPL became available for transfer to the *Surveyor* Project at HAC. A function of the data acquisition center is to make use of the computer data system to provide added telemetry data display during system test and to provide processing of these data for real-time and near-real-time analysis.

The computer data system from the *Mariner C* Project will be programmed and operated by JPL personnel. It will be an interim system supporting the testing of the SC-1 flight spacecraft at HAC and at the Air Force Eastern Test Range. It consists of a Univac 1218 computer with the necessary auxiliary equipment for accepting telemetry data and certain ground test data. The processed data are displayed in engineering units to the test team by means of a line printer and six character printers.

The final data acquisition center system will also be built around a small general-purpose computer. Generally, the final system will have more input data handling capability, faster and more extensive data processing, and greater data display capability. The system will have the capability of handling three spacecraft system tests being conducted simultaneously. Again, most of the system will be supplied, programmed, and operated by JPL. The scheduled operational date for the system is September 1965 for telemetry bit stream data handling, with full capability by early-1966.

PLANETARY–INTERPLANETARY PROGRAM

III. *Mariner* Project

A. Introduction

The early objective of the Planetary–Interplanetary Program is the initial probing of the planets Mars and Venus by unmanned spacecraft. The initial probing of Venus was successfully accomplished by *Mariner II*. The next step toward this objective is the initial probing of Mars by the *Mariner IV* spacecraft, which is now in transit.

The primary objective of the *Mariner C* missions (*Mariner* Mars 1964 Project) is to conduct closeup (flyby) scientific observations of the planet Mars during the 1964–1965 opportunity and to transmit the results of these observations back to Earth. The planetary observations should, to the greatest practical extent, provide maximum information about Mars. TV and cosmic dust experiments and a reasonable complement of field- and particle-measuring experiments are being carried by *Mariner IV*. In addition, an Earth occultation experiment is planned to obtain data relating to the scale height and pressure in the atmosphere of Mars.

A secondary objective is to provide experience and knowledge about the performance of the basic engineering equipment of an attitude-stabilized flyby spacecraft during flight in space farther away from the Sun than the Earth. An additional objective is to perform certain field and/or particle measurements in interplanetary space during the trip and in the vicinity of Mars.

The *Mariner III* (*Mariner C-2*) spacecraft was launched from the Air Force Eastern Test Range (AFETR) on November 5, 1964. The nose cone failed to eject from the spacecraft, thereby precluding solar-panel deployment; the battery power was depleted 8 hr, 43 min after launch.

The *Mariner IV* (*Mariner C-3*) spacecraft was successfully injected into a Mars encounter orbit about the Sun on November 28, 1964. All subsystems are performing as designed, with three exceptions: The solar plasma probe data are degraded due to a power supply failure which occurred after approximately 1 wk in flight; the Geiger-Müeller 10311 tube failed a few days after the solar flare

of February 5; and the ion chamber experiment failed on March 17 during the Johannesburg Tracking Station view period. No telemetry data were being received at the time of failure, since the Johannesburg Tracking Station was assigned to *Ranger IX* tracking operations at that time. Studies indicate that the failures of the Geiger-Müeller 10311 tube and the ion chamber both occurred within a common power supply. Thus far, there have been no detectable effects on the remainder of the spacecraft resulting from these failures.

The cosmic dust or micrometeoroid impacts upon the cosmic dust detector have shown a marked increase during this reporting period. The average rate has risen from 1 to 2 hits/wk shortly after launch to about 3 hits/day and is expected to increase even further. By comparing the area of the cosmic dust detector to that of the entire spacecraft, it is computed that, for each hit on the detector, there are 200 hits on the spacecraft. These impacts have had no detectable effect on the performance of any spacecraft subsystem.

By April 30, *Mariner IV* was in flight for 153 days, surpassing the *Mariner II* record of 129 days. On the same date, the communications distance (Earth-to-probe) was 67.4 million miles, surpassing all known communications distance records.

The *Mariner C-4* spacecraft (flight spare) and its associated operational support equipment have been returned to JPL, where the spacecraft will undergo a complete system test and then be placed in bonded storage.

B. *Mariner IV* Space Flight Operations

The following standard (planned) events were executed:

(1) Central computer and sequencer (CC&S) command MT-5 to switch the spacecraft transmitter to the high-gain antenna was issued at 064:13:02:40 GMT[1]. *Mariner IV* continues to receive on the low-gain antenna.

(2) CC&S command MT-2 to update the Canopus tracker cone angle was issued at 092:14:25:15. Two more steps of the Canopus tracker cone angle are planned before encounter.

Other than the three failures previously described, the nonstandard events which occurred were as follows:

(1) Disturbances in the roll channel of the attitude-control subsystem were observed on seven different days. No loss of Canopus intensity was observed.

(2) Fluctuations in the ground-received signal strength were observed; these were apparently due to interference patterns between the high- and low-gain antennas.

(3) Sudden drops in received signal strength coincident with the CC&S cyclic pulses were observed by the Deep Space Instrumentation Facility while in one-way lock.

(4) The spacecraft battery voltage continued to rise even though the battery charger was off. This anomaly was believed to have been caused by a slight trickle charge from the battery voltage transducer and unexpected sensitivity to small charge currents at a battery temperature between 60 and 70°F. A life-test battery is being operated at a lower temperature and a slightly higher voltage than the flight battery in an attempt to predict future operation of the *Mariner IV* unit. The test will continue until Mars encounter. The level is not expected to rise above 35.7 v, although the upper limit is presently 36.0 v.

(5) A 1-db decrease in average ground-received carrier power was observed approximately coincident with the MT-2 command on April 2.

C. *Mariner IV* Attitude-Control Subsystem Performance

1. Initial Sun Acquisition

The first function performed by the *Mariner IV* spacecraft was the reduction of the separation rates generated by the process of separation from the *Agena* booster. Since the spacecraft was injected into orbit while in the Earth's shadow, only gyro rate information was available,

[1]All times given here are GMT, day of year:hr:min:sec.

and the rate feedback reduced the rates to the deadband values: ± 1.27 mrad/sec in pitch and yaw and ± 0.33 mrad/sec in roll. When the spacecraft was first observed in the shadow, the rates were already within the deadband, indicating that the separation rates were very low.

When the spacecraft emerged into the sunlight, Sun sensors provided additional attitude-control information to reduce the position errors to the switching amplifier deadband values: ± 8.6 mrad. The actual time of exit from the Earth's shadow was 333:15:17:35, but Sun sensor signals were first noted at 333:15:16:37 due to the refraction of sunlight through the Earth's atmosphere.

When the spacecraft was fully in sunlight, the pitch error was seen to be −1.0 deg, and the pitch axis had essentially acquired. The yaw Sun sensors were saturated and had established a rate determined by this saturation equal to −2.2 mrad/sec (−0.126 deg/sec). The yaw sensors came out of saturation at 333:15:29:56.

A Sun gate event occurred at 333:15:30:59; the Sun gate cone angle field-of-view was 2.2 deg, which is within the design tolerance. The Sun gate initiated the magnetometer calibration spin as required. A search signal was switched into the roll-axis control system, and the spacecraft accelerated to a rate of −3.55 mrad/sec (−0.203 deg/sec), which is the design nominal. During the magnetometer spin mode, the pitch and yaw errors were observed to limit cycle against one side of the deadband. The pitch axis remained at the 8.7-mrad edge, and the yaw axis remained at the −8.5-mrad edge. This was as expected and was due to cross-coupling from the cross-products of inertia.

2. *Initial Star Acquisition*

Initial roll acquisition was commanded by the CC&S to occur at 334:06:59:00. At the roll acquisition command, the search command signal was switched in, and the roll rate was reduced to −2.35 mrad/sec (−0.135 deg/sec), which, as expected, was the upper value of the deadband search rate about the nominal. An acquisition occurred at 334:07:07:47. At that point, earthlight reflections on the star tracker optics caused a sufficiently bright background, along with a spurious error signal, to cause the acquisition logic to discontinue the roll search. Even though there was no acquirable object, a logic acquisition had been effected. The clock angle at that time was approximately 129 deg. (A graphical definition of clock angle and cone angle is given in Fig. 1.)

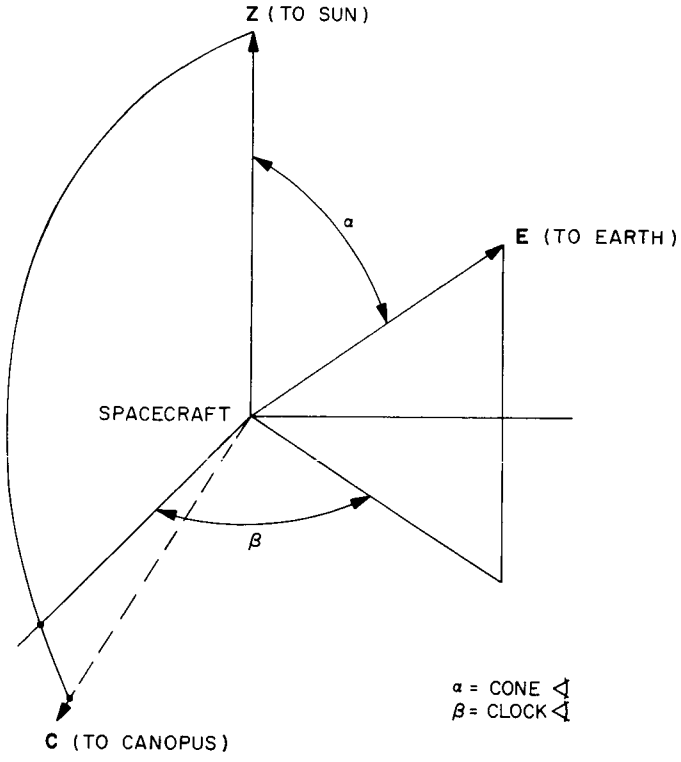

Fig. 1. Graphical definition of clock angle and cone angle

Even though the logic circuitry was satisfied, there was no real error signal, and the roll axis was essentially in a drift mode, with the jets firing at random due to background noise. This cumulative action caused the spacecraft to drift primarily in a direction of increasing clock angle. At some unknown time during the drift, the star Alderamin was acquired at a clock angle of 171 deg after drifting about 42 deg. Alderamin is about 0.05 times as bright as Canopus with a bright background, and the error signals were too noisy to determine the time of acquisition.

At 334:13:12:34, the spacecraft went into an automatic roll search. This loss of roll acquisition was the first of a series of losses of acquisition. Eventually, it was realized that these losses were caused by minute particles floating by and reflecting light into the tracker. At 334:13:26:15, after 13 min, 41 sec of roll search, the star Regulus was acquired at a clock angle of 278 deg. Lock was maintained on Regulus until the following day, since Canopus acquisition was not necessary until that time.

At 335:09:13:47, Direct Command (DC) 21 (roll override) was initiated. The star Naos was acquired at 335:09:20:56 at a clock angle of 338 deg. Another DC-21

at 335:10:45:09 caused γ Velorum to be acquired at a clock angle of 343 deg at 335:10:46:00. Then, Canopus was acquired by a DC-21 initiated at 335:10:57:57, and lock was obtained at 335:10:59:38.

3. Solar Vane Acquisition

The first solar vane measurements were coincident with the turn-on of the adaptive mode actuators at the time of the initial star acquisition. At that time, it was noted that the vanes had been deployed beyond the nominal position angle of 35 deg below the plane of the solar panels. They were deployed in the following positions: $+x$ vane at 21 deg, $-x$ vane at 15 deg, $+y$ vane at 17 deg, and $-y$ vane at 11 deg. The deployment failure was due to an unsuspected source of friction that was present during ground testing, but not present in the space environment. In spite of the overtravel, the center of pressure of the spacecraft was behind the center of gravity, so there was a net restoring torque of about 1.1 dyne-cm/deg about the pitch axis and 1.7 dyne-cm/deg about the yaw axis.

The $+x$ and $-x$ vanes, which control the yaw axis, were working properly in the adaptive mode by cancelling out an initial unbalanced torque of about 25 dyne-cm, probably due to the skewed angle of the high-gain antenna. The $+y$ and $-y$ vanes were definitely in a failed mode. The most likely explanation was that the actuators were locked up electrically. The design is such that, within the first 30 msec of actuator turn-on, if a gas jet fires, the actuator will lock. The telemetry data indicate that it is very likely that a jet did fire at that time.

Since the $+x$ and $-x$ vanes were operating in the adaptive mode to reduce the unbalanced torques, they were expected to eventually operate in the thermal mode to damp out the limit cycle. It immediately became apparent that, after the unbalanced torque was reduced to about 5 dyne-cm, the disturbance torques were quite variable. It was not possible for the thermal actuators to perform their function under those circumstances. The varying disturbance torques were obviously not solar torques. The best explanation thus far is that they were due to the normal leakage of the gas valves.

The normal valve leakage of 3.0 cm^3/hr at standard conditions will actually provide 16 dyne-cm of torque per valve, if it is assumed that the nominal gas laws apply. There are four valves controlling each axis, and the leakage was observed in tests to vary with valve actuation. Therefore, even though the average leakage is known, the leakage and, hence, the torques could vary considerably over a period of time. If the seating characteristics of the valves change over a period of time, long-term variations in the disturbance torques would be expected, and, if the seating for each valve firing is slightly different, then short-term variations could be seen. The long-term disturbance torques varied, and the $+x$ and $-x$ vanes were observed to be moving and cancelling out these disturbances in the adaptive mode of operation.

4. First Midcourse Maneuver Sequence

The midcourse sequence (initiation of DC-27) began at 339:14:35:00. DC-27 turned on the gyros for warmup 1 hr prior to the start of the commanded turns. At 339:14:35:47, the gyros came on and started to spin up. The spinup of the gyros caused a disturbance in the attitude-control subsystem, and the pitch, yaw, and roll error signals were driven over to one side of the deadband. The roll channel, which is of particular interest, started limit cycling against the negative side of the deadband with an angular excursion of 1 data number, which is a resolution of 0.41 mrad. After 49.3 sec of operation (11 frames of data), a large transient was observed in the roll error channel equivalent to -16.0 mrad. The next data frame (4.2 sec later) showed the spacecraft going into automatic roll search, which continued until earthlight reflections caused an acquisition to occur at 339:14:52:32 at a clock angle of about 90 deg.

The roll error signal being forced to one side of the deadband by the gyro spinup was a normal event. The huge transient in the roll channel (and subsequent loss of acquisition) was prohibitive to the initiation of the maneuver and caused it to be postponed for 1 day. The one sample in roll error of -16.0 mrad was impossible to explain by actual spacecraft motion, because the impulse would have been "catastrophic" and would have been observed in the pitch and yaw channels and on the roll gyro, which it was not. It appears that the signal was an electrical transient of some kind.

It is postulated that the time correlation of gyro warmup to the subsequent loss of acquisition was due to the fact that the particles which were shaken loose from the solar panels by the gyro starting transient were then driven in front of the star tracker by solar pressure or spacecraft static charge. An instantaneous bright flash would cause a high brightness gate violation and a false error signal. Since the resolution of events in this mode was 4.2 sec, it was possible to miss getting an indication of the flash in the brightness channel.

The performance of the spacecraft at the initiation of gyro warmup prior to the start of the second and successful midcourse sequence was identical to that prior to the first, except for the loss of acquisition.

5. Second Midcourse Maneuver Sequence

The second midcourse maneuver sequence began at the initiation of DC-27 at 340:14:25:13. The gyros came on, and the gyro spinup caused the roll limit cycle to stay on the negative side of the deadband, as in the first maneuver try. (This is normal operation.) After the gyros were up to speed, the roll limit cycle was normal.

The maneuver consisted of a pitch turn of −39.16 deg and a roll turn of 156.07 deg. The pitch turn starting transient was seen at 340:15:25:12 and the stopping transient at 340:15:28:54. The roll turn starting transient was seen at 340:15:47:10 and the stopping transient at 340:16:01:19. The turns were correct in every respect. The amount of overshoot in the rate-plus-position measurement during the starting and stopping transients was within the tolerances for the given control system acceleration of 0.45 mrad/sec. This is the only good confirmation available of the steady-state operation of the gas jets.

The turn angles included a small adjustment in pitch and roll to compensate for a known center-of-gravity misalignment error. A small adjustment was also made to the motor-burn time to compensate for jet-vane drag. The compensation was based on the predicted initial conditions to the autopilot from the attitude-control subsystem. On the basis of the commanded turn angles, it was expected that solar torques would keep both pitch and yaw angular positions held against the negative side of the attitude-control deadband. The actual position of the spacecraft in the pitch and yaw attitude-control deadband was exactly as predicted.

The midcourse rocket, ignited at 340:16:09:09.6, burned for 20.4 sec. Four data points on the gyro signals were received during the motor-burn period. Although these did not provide enough data for a thorough analysis, three significant events appear to fit the observed points: (1) The first data point after motor ignition indicates a transient overshoot in pitch and yaw (expected from the known, initial conditions on the autopilot); (2) for the remaining three points during the burn period, pitch and yaw maintained an equal and opposite offset, indicating a center-of-gravity misalignment angle of approximately 2.2 mrad; and (3) a very slow motion in the roll channel may have been a low-amplitude limit cycle due to friction in the jet-vane actuators. This limit cycle, theoretically predictable, has been observed in analog computer simulations, but has not been observed in previous spacecraft because of insufficient data during the midcourse maneuvers.

Performance of all subsystems during the entire midcourse maneuver was very satisfactory. Tracking data have verified that the *Mariner IV* midcourse maneuver was very accurate.

6. Reacquisitions After Midcourse

Sun reacquisition was commanded by the CC&S at 340:16:15:10. Since the pitch turn was of such a small magnitude, the Sun acquisition was short, taking place at 340:16:21:07. Again, the Sun gate field-of-view was seen to be 2.2 deg.

The Sun gate event started roll search for Canopus, and the first star acquired was γ Velorum at 340:16:44:36 at a cone angle of 342.8 deg. Roll override was initiated at 340:16:52:50, Canopus was acquired at 340:16:55:00, and regular roll control was established.

7. Cruise

a. Roll-control transients. During the attitude-control cruise portion of the flight, it was observed that transients in the roll-control system caused the spacecraft to go into the automatic roll-search sequence. In some cases, a brightness transient in the star tracker was associated with the roll-error transient. Five of the roll transients were noted in the first 10 days of flight. It was determined that the most probable cause was minute bright particles which were floating by the Canopus tracker and causing brightness transients which exceeded the upper brightness gate limits of the tracker. If the error signal in the tracker were negative, reacquisition would take place immediately; otherwise, the automatic roll search took place. An investigation to locate a possible mechanism for the generation of particles showed that extremely small meteoroids (approximately 10^{-3}g) impacting the spacecraft could cause the release of dust and lint in frequency of occurrence in the range to explain the observations.

It was recommended that DC-15 be used to remove the high gate from the control system logic circuitry. This was accomplished at 352:17:30:00. As of April 9,

1965, the use of DC-15 has been very successful. Many roll transients have been observed, but none has caused a loss of acquisition.

b. Attitude-control gas consumption. The gas consumption during the cruise mode is 3.76×10^{-3} lb/day $\pm 10\%$. As of April 1, the total weight remaining was 4.68 lb, yielding a lifetime of 3.4 yr as of that date. This is well over the requirement.

D. Development of a Star Identification Procedure

Before the flight of *Mariner IV*, it was felt that star identification would be a major problem since the only information from the star tracker, other than an error signal, is a brightness measurement and the cone angle of an object within ± 5 deg. The absolute calibration of the star tracker for all stars is not known, and the problem is further complicated by the brightness signal including the integrated background of stars in the field. But, during the roll-search mode, the tracker makes good relative measurements of the star-plus-background brightness. This information is basic to the star identification procedure.

A map-matching technique was developed to identify objects seen by the star tracker during the roll-search mode. As an aid to establishing the map-matching technique, other corroborating information was used for initial acquisition: a fixed wide angle (26- $\times$ 83-deg) field-of-view Earth detector to provide an output if Canopus were in the star tracker, magnetometer information obtained during the calibration mode for rate and position information, and low-gain antenna pattern variations to provide rate and position information. The magnetometer and antenna data are very crude and can be used only with a low weighting function on their corroboration.

Fundamental to the map matching was an *a priori* telemetry map of tracker brightness output versus clock angle (angle about the Sun line measured from Canopus). A reasonably sophisticated mathematical model of the star tracker and the sky, including the Milky Way, was developed so that, with the trajectory information, an IBM 7094 computer program printed a map of the expected telemetry output of the brightness channel seen during roll search. This then could be matched with an actual telemetry map to identify observed objects.

Initially, an extensive computer program was devised to process the telemetry data to produce the actual telemetry map. This was statistically correlated with the *a priori* map, Earth detector output, magnetometer data, and low-gain antenna data. Whenever an object was acquired subsequent to a roll search, a calculation was made of the probability that each acquirable object had been acquired. If the object were not Canopus, roll override would institute another roll search, and another computer run was made until Canopus was identified as acquired.

The computer-generated version of the map matching was necessary, due to the lack of knowledge of the tracker response to innumerable objects and the integrated background that would be seen by the tracker. Until the tracker could actually be calibrated in flight, the uncertainties required that the best possible analysis techniques be prepared beforehand.

In addition to the computer-generated star identification program, a second map-matching technique was developed and implemented during the flight. This second technique was much simpler, but required actual flight experience to prove reliability. A continuous strip chart recorder was employed to plot, in real time, the star tracker brightness telemetry. An *a priori* map derived from the computer program was transcribed to a transparent overlay to the same scale as the real-time telemetry plot, so that they could be instantaneously compared during the roll search. The process proved to be very satisfactory and became the primary technique for star identification. It was quite accurate and the fastest possible means for identifying objects. The development of the procedure consisting of excellent *a priori* maps matched in real time with brightness telemetry data is felt to be one of the *Mariner IV* mission accomplishments.

DEEP SPACE NETWORK

IV. Deep Space Instrumentation Facility

A. Introduction

The Deep Space Instrumentation Facility (DSIF) utilizes large antennas, low-noise phase-lock receiving systems, and high-power transmitters located at stations positioned around the Earth to track, command, and receive data from deep space probes. The DSIF stations are:

Station	Location
Goldstone Pioneer	Goldstone, California
Goldstone Echo	Goldstone, California
Goldstone Venus (research and development)	Goldstone, California
Goldstone Mars (under construction)	Goldstone, California
Woomera	Island Lagoon, Australia
Tidbinbilla	Canberra, Australia
Johannesburg	Johannesburg, South Africa
Madrid (under construction)	Madrid, Spain
Spacecraft Monitoring	Cape Kennedy, Florida
Spacecraft Guidance and Command (under construction)	Ascension Island

To improve the data rate and distance capability, a 210-ft-diameter Advanced Antenna System is under construction at the Goldstone Mars Station, and two additional antennas of this size are planned for installation at overseas stations. Overseas stations are generally operated by personnel of the respective countries.

It is the policy of the DSIF to continuously conduct research and development of new components and systems and to engineer them into the DSIF to maintain a state-of-the-art capability.

B. Tracking Stations Engineering and Operations

1. Goldstone Pioneer Station

The Goldstone Pioneer Station provided receiver backup and recovery of video during the *Ranger IX* mission. In the period between the *Ranger VIII* and *IX* missions, the acquisition time of *Mariner IV* had advanced sufficiently that the Pioneer Station was able to transfer the *Mariner IV* track to the Tidbinbilla Tracking Station at the approximate time of acquisition of *Ranger IX* by the Goldstone Echo Station. The change from S- to L-band was accomplished in less than 2 hr.

With the conclusion of the *Ranger* Project, the L-band systems at both the Echo and Pioneer Stations are being dismantled and stored.

The tracking of the *Mariner IV* spacecraft is continuing on a routine basis. On March 5, the spacecraft central computer and sequencer switched the transmitter from the low- to the high-gain antenna. In preparation for the occultation experiment to be performed during Mars encounter, preliminary tests were conducted to establish the compatibility of the occultation equipment with the S-band system. Additional tests are scheduled to ensure operational readiness.

The following DSIF/*Surveyor* Project compatibility tests were performed between *Mariner IV* tracking periods: (1) initial tests of the FR-1400 recorder's capability to record *Surveyor* low-level subcarrier oscillators, (2) leakage tests of the *Surveyor* transponder, and (3) command word error tests. Testing of the on-station data processing equipment interface is in progress.

2. Goldstone Echo Station

The L-band equipment at the Goldstone Echo Station was maintained in an operational status between the *Ranger VIII* mission and the launch of *Ranger IX*. Two operational readiness tests were conducted. *Ranger IX* was commanded to change from the low- to the high-gain antenna during this station's first view period, the midcourse maneuver was performed during the second view period, and the terminal maneuver was performed during the third view period.

Completion of the *Ranger* Project and the phase-out of the L-band system placed increased emphasis on the installation of the S-band system to provide additional backup to the Goldstone Pioneer Station during the forthcoming *Mariner IV* Mars encounter. In preparation for the installation, an S-band wing (Fig. 1) was added to the existing control building. Occupancy of the building began soon after the completion of the *Ranger IX* mission when portions of the new S-band receiver were moved into the new wing. The portions of the L-band equipment that could be used in the S-band system were removed for quality-control inspection and for modifications if needed. The equipment is being installed as it becomes available.

Structural modifications to the transmitter and receiver cages are in progress on the antenna. The receiver cage is being relocated on the east side of the reflector to provide easier access to the equipment from the ground. No major structural changes are being made to the antenna due to the limited time remaining before the *Mariner IV* Mars encounter.

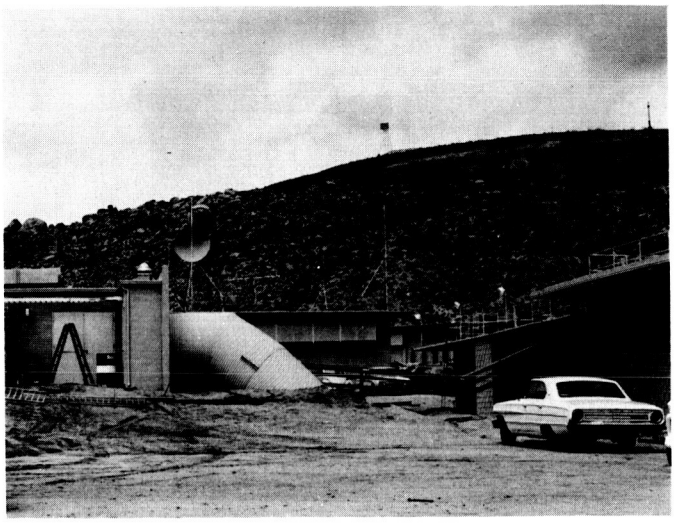

Fig. 1. Antenna side of new Goldstone Echo Station control building S-band wing

3. Goldstone Venus Station

After the successful *Mariner IV* tracking operations during the third view period for *Ranger VIII*, additional test tracking was performed. Two-way coherent and three-way noncoherent doppler between the Goldstone Pioneer Station, Goldstone Venus Station, Tidbinbilla Tracking Station, and the spacecraft was obtained. Microwave interfaces between the Venus and Pioneer Stations are still being optimized.

Final system testing of the *Mariner IV* exciter was performed. The command loop between the Venus Station and the *Mariner IV* spacecraft was successfully locked and command modulation applied; however, no commands have been transmitted to the spacecraft from the Venus Station. The *Mariner* system is operationally ready for Pioneer Station backup support.

4. Ranger IX Tracking Operations

Due to the uprange injection of *Ranger IX*, the Woomera Tracking Station would have short or nonexistent view periods on the first pass, depending upon the launch day. Considering antenna angular constraints,

the nearest the Woomera Tracking Station would come to a view period would be with the spacecraft 4 deg away from its main beam. Since Woomera could not transmit on the acquisition aid, preflight studies were made of the power in the transmitter side lobes to determine if two-way doppler could be obtained from the station if necessary. These studies indicated that two-way lock at the station on the first pass was possible, but should be attempted only if the Johannesburg Tracking Station experienced doppler problems.

The first DSIF station to track *Ranger IX* was the Spacecraft Monitoring Station, which acquired the spacecraft prior to launch and tracked it from launch to the horizon, taking telemetric data only. A trajectory seen by this station is a function of launch azimuth only; therefore, new preflight predictions were not generated for *Ranger IX*. A new offset frequency was provided to compensate for the difference in frequencies between *Rangers VIII* and *IX*. The Spacecraft Monitoring Station tracked *Ranger IX* for 7 min, 35 sec, several seconds below its horizon mask.

The Johannesburg Tracking Station acquired the spacecraft within 20 sec of its first view period. The acquisition was made with the ground transmitter on; therefore, when ground receiver lock was established, two-way lock was also established. The orbit-determination process used at JPL is very sensitive to data near injection. By acquiring the spacecraft in a two-way mode, two-way doppler is obtained as near injection as possible. These data are of great value in quickly obtaining a good orbit determination. The Johannesburg Tracking Station was taking two-way doppler data within 20 sec from the start of the view period.

Approximately 13.5 min after the first acquisition at 080:22:14:44 GMT[1], the Johannesburg Tracking Station switched the transmitter exciter chain from a voltage-controlled oscillator (VCO) to a rubidium-standard-controlled frequency synthesizer. Tests on *Ranger VIII* had shown that two-way doppler data had less noise when the synthesizer, rather than the VCO, was used as the frequency source. On *Ranger IX*, however, the data noise increased when the synthesizer was used, so it was decided to have the station return to the VCO. This was accomplished at 080:22:36:06, and the noise decreased. The station then changed synthesizers and took data, using the new unit, between 080:22:55:15 and 080:23:12:10. When these data also were found to contain excess noise, it was decided that the Johannesburg Tracking Station should change its rubidium standard. Since it was necessary for this station to interrupt tracking momentarily to make this change, the Woomera Tracking Station went into a two-way mode during this period. When Johannesburg reacquired two-way lock at 081:00:25:20, the data noise had been reduced, and it remained at a reduced level for the rest of the pass. There was a time bias on the doppler data from 081:00:25:20 to 081:00:40:13 due to the changing of the rubidium standard. Although analysis is not yet complete, it appears that the rubidium standard was the cause of the noise.

A midcourse maneuver was executed during the Goldstone Echo Station view period on March 23. Motor ignition occurred at 082:12:30:10 and motor shutoff at 082:12:30:40. The total doppler shift was 88.5 cps, indicating a radial velocity shift of 13.8 m/sec as compared to the nominal velocity input of 13.97 m/sec. The spacecraft was tracked throughout the burn period in a two-way doppler mode.

Due to the trajectory of *Ranger IX*, the possibility arose that the Woomera Tracking Station could "see" lunar impact. An extra set of predictions was generated and indicated that the spacecraft would impact before it would rise within the main beam of the Woomera antenna, which was constrained by 270-deg hour-angle limits. A squint feed was installed at the station to change the angle of the main lobe away from the central axis of the paraboloid. This was accomplished by moving the feed so that the angle of illumination was changed. The Woomera Tracking Station acquired the spacecraft 25 min before impact, but dropped lock at 083:13:58 when the Goldstone Echo Station transmitter failed. The Goldstone Echo Station receiver dropped lock, but recovery was rapid, with only 1 min of tracking data being lost. Because the voice net to Woomera was tied in to the public information net which was giving TV subsystem information, the station was not promptly notified of the transmitter failure. Thus, the spacecraft was not acquired by Woomera during the last 10 min before impact.

An experiment to measure the exact time of lunar impact was conducted at the Goldstone Echo Station. The experiment consisted of counting the station's 1-Mc reference frequency, using the 1/min station time pulse as the start trigger and the decaying spin modulation output as the stop trigger. The spin modulation output (unfiltered coherent automatic-gain-control voltage) is precalibrated and postcalibrated to measure the receiver delay. Receiver delay uncertainty has been the limiting factor in impact-time measurements. Analysis shows the 1-σ uncertainty to be 185 μsec. Impact (loss of carrier) of

[1] All times given here are GMT, day of year : hr : min : sec.

Ranger IX was recorded at 083:14:08:21.325916 ±185 μsec. A second impact time was recorded by passing a 2-Mc spacecraft signal through a 300-kc filter along with the NASA 100-pps signal and a 1-Mc signal. This method showed the impact time to be 083:14:08:21.325864 ±7 μsec. Both times are uncorrected for wave-propagation time, which is estimated to be 1.32704 sec. The second method is more accurate than the first, but has the disadvantage of an approximately 2-wk reduction time, as compared to the instant readout and ½-hr calibration necessary for the first method. The two methods agree, however, since the second time is nested within the stated uncertainty in the first.

C. Developmental and Testing Activities

1. S-Band Test Antenna

The S-band test antenna (Fig. 2), used to make gain, pattern, and ellipticity measurements on DSIF antennas, is made up of the following equipment: (1) a reflector assembly, (2) a circular-aperture feed assembly, and (3) a control panel. The reflector assembly consists of an 8-ft-D paraboloidal reflector with focal-length-to-diameter ratio of 0.375, a mounting structure which provides a ±5-deg adjustment in both azimuth and elevation, an optical boresight telescope with protective housing, and a spar and horn ring structure for feed support.

The feed assembly contains a dipole and coaxial rotary joint with a ⅞-in. coaxial output, an iris section which acts as a polarization transducer, a drive motor for changing and orienting polarizations, two synchro-transformers (1:1 and 36:1 gear ratios), logic switches for control and readout of polarization changes, and a weatherproof housing and radome.

The control panel consists of a 19- × 10.5-in. panel with operating controls and a dial indicator for polarization orientation readout, a power supply, motor speed control, and 150 ft of connecting control cable.

The antenna is installed near the top of the standard DSIF collimator tower, and the polarization control panel is located in the collimation microwave cabinet at the base of the tower. The S-band test antennas have been in operation at DSIF stations since July 1963 and have experienced only one failure: a defective microswitch in the feed unit of one of the overseas antennas.

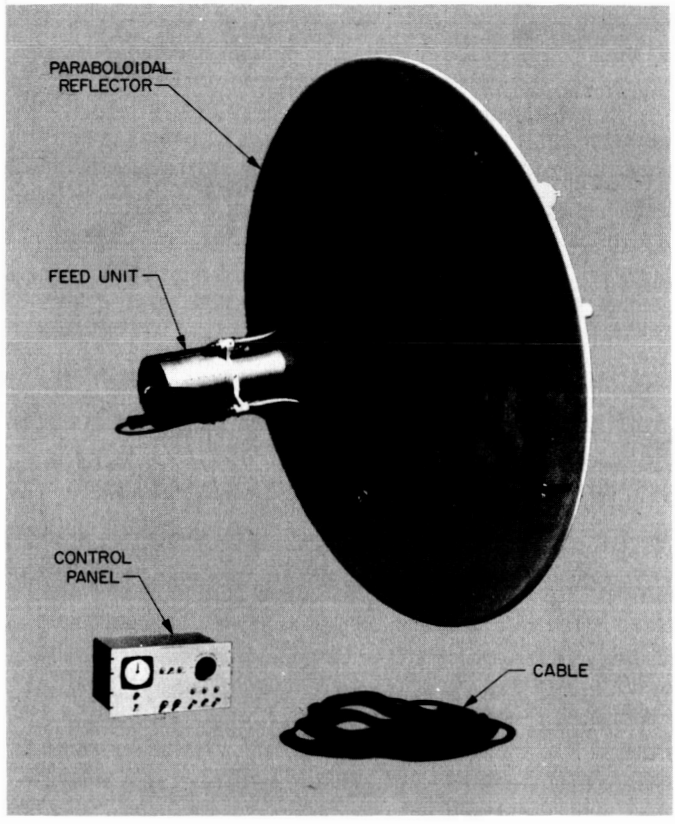

Fig. 2. S-band test antenna

2. Coherent Frequency Translator

Self-checking, a capability of the receiver–exciter subsystem, is accomplished by translating a sample of the exciter signal to the receiver frequency. The exciter characteristics can then be examined with the receiver and the receiver calibrated with the exciter. In the Deep Space Network (DSN) 1964 S-band receiver–exciter subsystem (*SPS 37-28*, Vol. III, pp. 30–39, and *SPS 37-32*, Vol. III, pp. 10–19), this was accomplished by combining a sample of the exciter signal with a signal generated from a crystal oscillator. The primary disadvantages of this mechanization were: (1) The oscillator crystal had to be changed each time the exciter was moved from one frequency channel to another; and (2) since the derived receiver frequency was not coherent with the exciter, there was no capability for performing coherent tests.

To remove these limitations, a coherent frequency translator was developed for use in the Manned Space

Flight Network (MSFN) and DSN subsystems. The improved design consists primarily of two new subassemblies: the translator module (Fig. 3) combining the two frequencies and a $\times 32$ frequency multiplier module generating the coherent reference signal. The coherent relationship between the receiver frequency and the transmitter frequency is 240/221. A coherent reference signal related to the exciter by the factor 19/221 is derived and combined with a sample of the exciter signal to obtain the coherent receiver frequency.

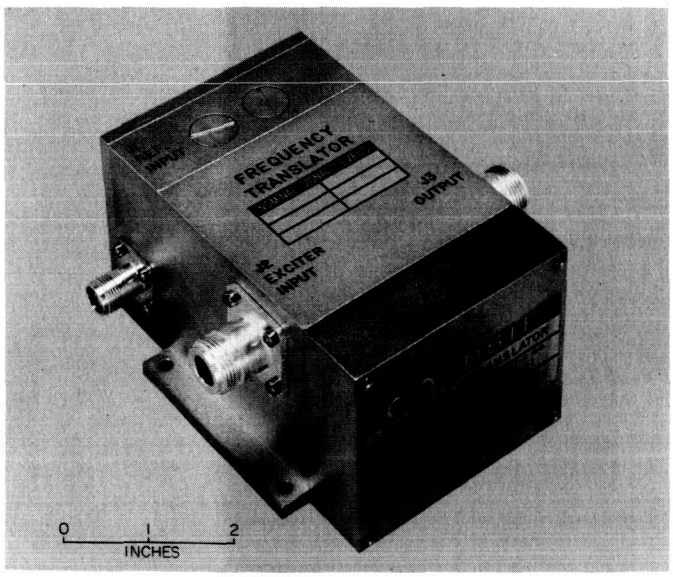

Fig. 3. Translator module

In addition to obtaining the capability for coherent translation, the performance of the translator was extended in other areas, namely: an increase in the dynamic range, an increase in the bandwidth to cover the coherent portion of the MSFN band and the DSN band, the addition of a high-level power monitoring output, and improved shielding to permit calibrations down to threshold levels.

3. Mariner IV Encounter Receiver

The *Mariner IV* support at the Goldstone Venus Station includes (in addition to the 100-kw transmitting capability and the "suitcase" telemetry reception for *Mariner IV* during the flights of *Rangers VIII* and *IX*) a low-noise, narrow- and broad-band flexible receiving capability for use during the *Mariner IV* Mars encounter phase. This capability will be achieved by the use of planetary radar techniques and hardware, adapted to the operational frequency and telemetry requirements. In addition to telemetry reception from just prior to encounter to several weeks thereafter, it is planned to record the received spectrum during the period of occultation for later analysis in conjunction with a similar experiment to be conducted simultaneously at the Goldstone Pioneer Station.

The present Mod IV lunar and planetary radar receiver will be used extensively in this application. Except for the programmed local oscillator, which is to be slightly modified, the balance of the equipment (including an antenna-mounted S-band to 30-Mc converter and a one-bay rack containing the local oscillator components and a commercial frequency synthesizer) will be specially installed. Two open-loop modes for occultation and three basic telemetry modes offer a high degree of reliability because of the equipment and the ability to optimize local oscillator purity with respect to signal strength and *a priori* doppler data. To minimize operating difficulties, the various controls have been interlocked to provide panel selection of any one of the five basic modes and to provide independent selection of two loop bandwidths for telemetry. Standard loop bandwidth is provided, with oscillator tracking ranges and stabilities comparable to those of the DSIF. In addition, it is expected that postencounter tracking with one-way doppler will be extended to the limit of the capability of a 5-cps threshold. This will be implemented in two ways: (1)The high-Q low phase noise voltage-controlled oscillator (VCO) of the lunar and planetary radar will be used, with doppler offset accomplished by the programmed local oscillator; and (2) as an alternate, three similar high-Q VCOs will be available on center frequencies selected by means of the trajectory data presently available; each will track unassisted over a comparatively narrow range.

Preliminary system testing has been completed on all new equipment except the high-Q VCOs, using the S-band transponder ranging station at JPL instead of the required portions of the Goldstone Venus Station Mod IV receiver. Final assembly of the special bay, utilizing the prechecked subsystem, is presently being accomplished. The antenna cone equipment (power supply, cabling, and converter mockup) was installed during January while the maser and waveguide modifications were being made.

SUPPORTING ACTIVITIES

V. Environmental Test Facilities

A. Modifications to a Refrigerant Valve for Increased Reliability at Cryogenic Temperatures

The vacuum systems in the JPL Environmental Test Laboratory (ETL) are equipped to provide, in addition to vacuum, a stable temperature environment adjustable between −300 and 275°F. Liquid nitrogen is the coolant used to provide the necessary cryogenic temperatures. The flow of liquid nitrogen through these systems is controlled by solenoid-operated valves that must be capable of functioning reliably at −320°F.

When the first vacuum-temperature control system was installed at JPL, there were no solenoid-operated, cryogenic-rated valves available commercially. The decision was made to use a valve in common use on most refrigeration systems. The manufacturer's specification indicated that the operating range of these valves was from −40 to 300°F. For some time, these valves operated reasonably well at cryogenic temperatures.

About once every 2 months, a valve would freeze and malfunction, resulting in the loss of temperature control for the operating vacuum system. Under such conditions, the specimen being vacuum-temperature-tested might be

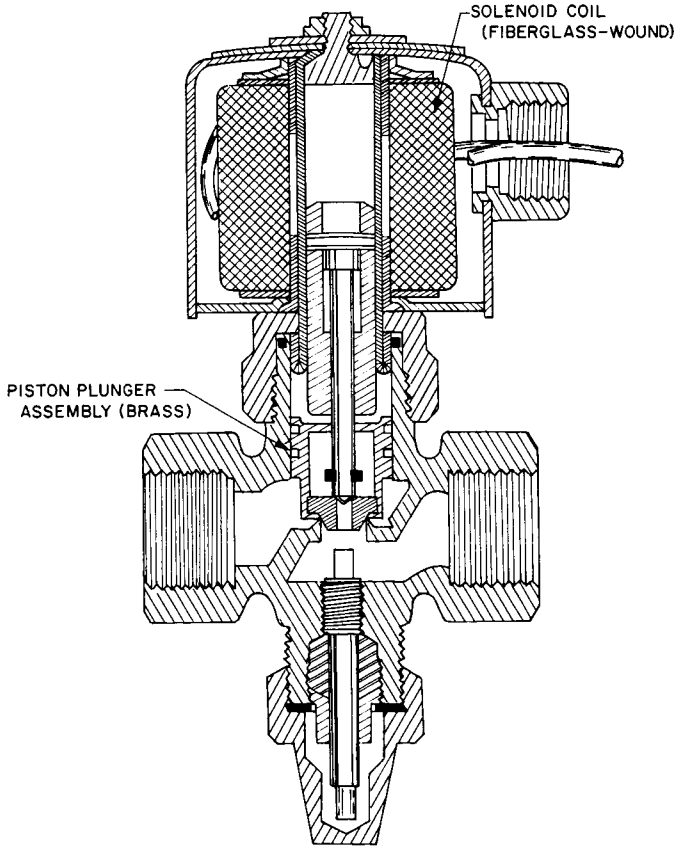

Fig. 1. Modified refrigerant valve

severely damaged by exposure to the temperature of liquid nitrogen, i.e., −320°F. The problem was temporarily solved by clamping a 47-w heater to the body of the valve. These heaters, however, periodically burn out, leaving the valve susceptible to later freeze-ups.

In addition to the malfunction due to freezing, the solenoid coils would periodically short-circuit and, in some cases, burn. Apparently, the contraction and expansion caused by the temperature changes in the coil caused the varnish-coated surface to crack, thus allowing water to enter into the interior of the coil. The water would freeze again, causing further deterioration of the insulation. Coil burnouts occurred approximately once every month.

The manufacturer indicated interest in JPL's problems with the valves. Predicated on the theory that the difference in the coefficient of expansion resulted in piston-body dimensions that were too close, the manufacturer provided two prototype internal parts kits for evaluation. These kits substituted brass for stainless-steel in the valve piston. To overcome the problem of the solenoid coil short-circuits, the manufacturer recommended replacing the standard cotton-wound coils with their fiberglass-wound ones (Fig. 1).

These modifications were made on two valves for the purpose of evaluation. A special test was set up (Fig. 2) to subject the modified valves to an environment more rigorous than is available on the JPL vacuum-temperature

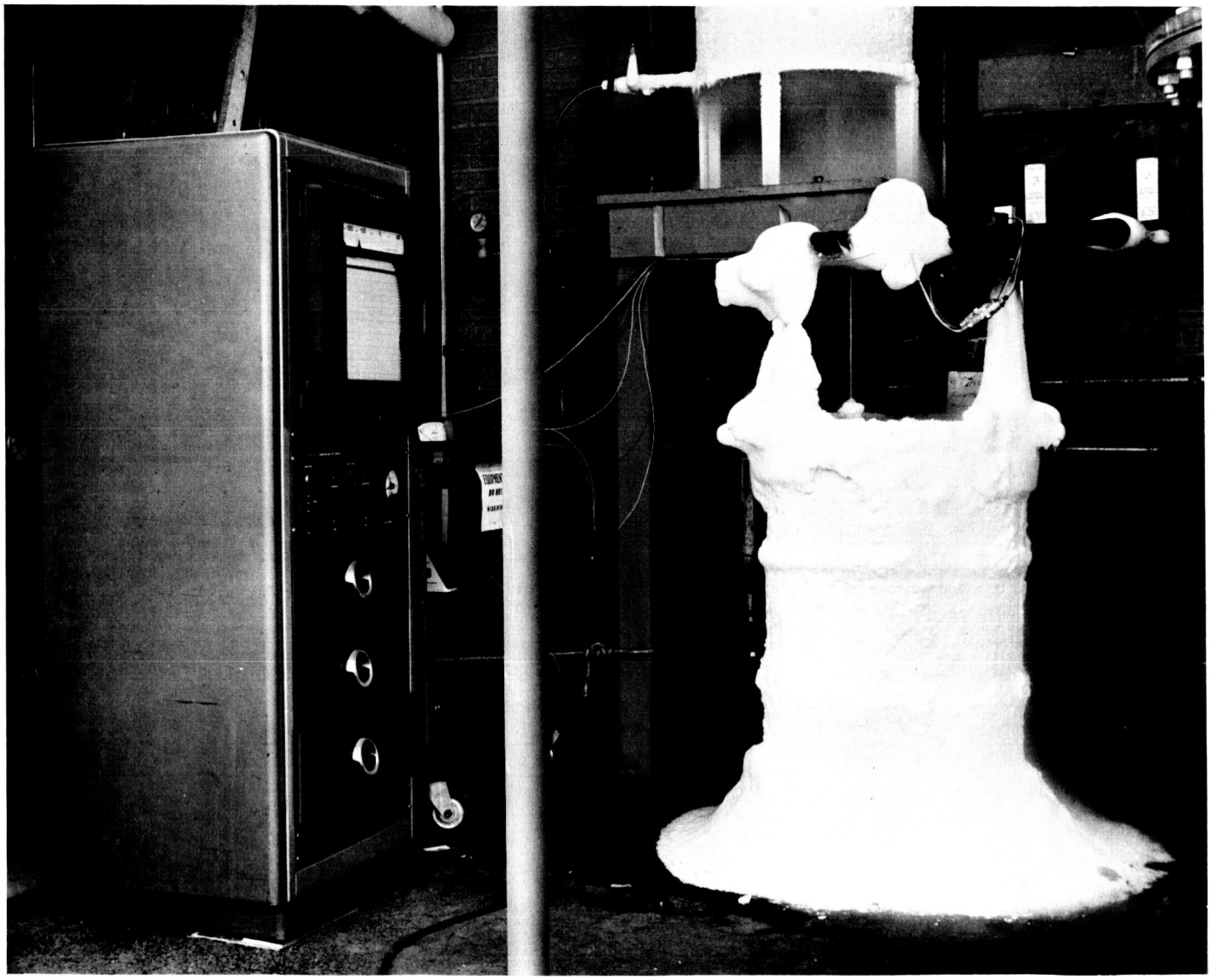

Fig. 2. Refrigerant-valve test setup showing icing conditions

control systems. The test was conducted 8 hr/day over a 5-month period, and all factors considered significant were carefully monitored. Fig. 3 shows the details of the test setup.

Neither valve failed during the test. Microscopic examinations of the valves were made after the test, and no signs of serious wear or deterioration were found. The internal parts and solenoids were returned to the manufacturer for further evaluation. In the test, it was established that the modified valve will reliably operate for extended periods in cryogenic service. From examination of the condition of the test valves, it is apparent that they should perform as long and as reliably as the unmodified valve version does under non-cryogenic service, i.e., 2 to 3 million operations.

Since the test results were favorable, the manufacturer has agreed to make internal parts kits for substitution in the JPL ETL vacuum systems. These cryogenic valves will also be available commercially.

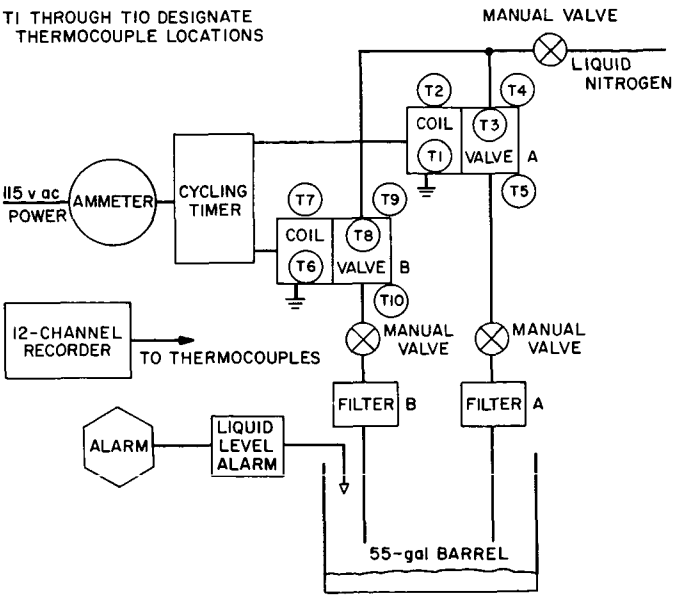

Fig. 3. Block diagram of refrigerant-valve test setup

SPACE SCIENCES

VI. Space Instrument Systems

A. *Mariner II* Data-Automation-System Life Testing

1. Data Automation System (DAS) Description

a. Functional. The *Mariner II* science payload was designed to: (1) make a number of interplanetary measurements, and (2) measure the planet environment at Venus encounter by radiometric means. The DAS that was used for the *Mariner II* mission is a solid-state digital electronic system designed to gather information from the scientific instruments on the spacecraft and prepare the information for presentation to the telemetry for transmission. The basic functions performed by the DAS for the instruments are analog-to-digital (A/D) conversion, digital-to-digital (D/D) conversion, sampling and instrument calibration timing, and planetary acquisition.

The transformed data are loaded into an eight-stage shift register, which is the center of the data-handling portion of the DAS. This register acts as a counter for the A/D conversions, a buffer storage for the D/D conversions, a pseudonoise generator for subframing and framing of the data, and a comparator for the planetary acquisition function. The 12 analog voltages sampled are from the magnetometer, the solar plasma experiment, infrared (IR) and microwave radiometers, and three temperature sensors. Digital data are received from the ionization chamber, particle flux detectors, the cosmic dust experiment, the magnetometer scale indication circuitry, and the solar plasma power-on indicator. The information is transformed by counting pulses, making time interval measurements between pulses, and direct parallel transfer. The data appear at the output of the DAS in a 21-word, 8-bits/word sequence. A functional diagram is shown in Fig. 1.

A binary clock and associated matrix logic are used to generate sampling intervals, reset commands, and scientific instrument calibration sequences. The binary clock is driven by a bit synchronization pulse from the spacecraft data encoder.

Detection of the planet by means of the microwave radiometer is accomplished by comparing the digital recording of the analog signal from the instrument with the digital equivalent of two voltages. If the analog voltage goes above 1.5 v, the scan speed is switched to slow speed. When the voltage has exceeded 2.25 v and then drops

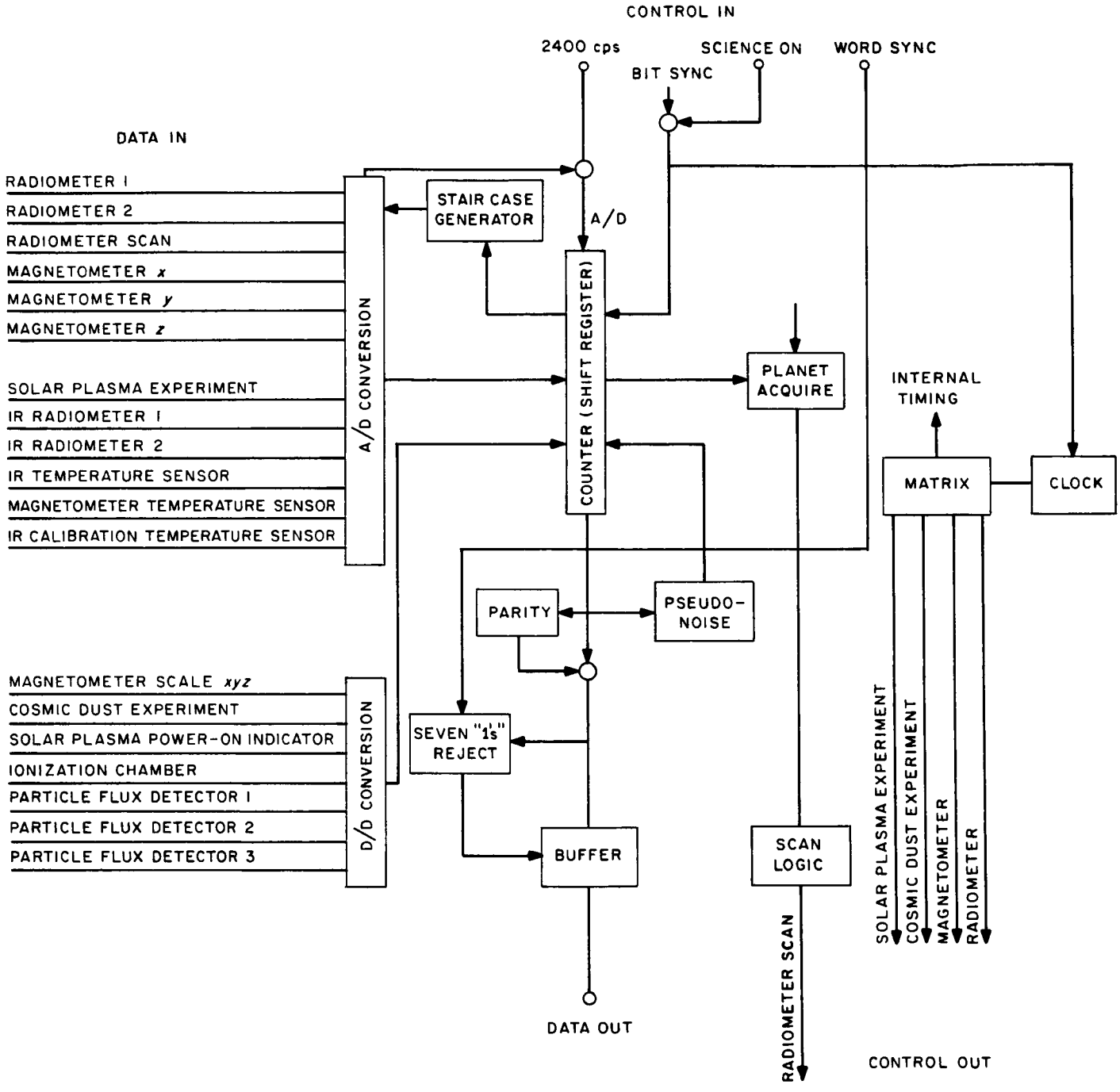

Fig. 1. DAS functional block diagram

below 1.5 v for more than 20 sec, the scan direction is reversed. If the analog voltage remains below 1.5 v for more than 160 sec, the scan is switched back to fast speed.

b. Assembly. The DAS is mounted on four standard 6- × 6- × 1-in. castings. The transformer–rectifier power supply is mounted on a half-size casting. The DAS and transformer–rectifier units employ 343 transistors, for a total of 3155 components with a total weight of 6.6 lb. The system requires 2.2 w of raw power from the spacecraft power system. The DAS assembly is shown in Fig. 2.

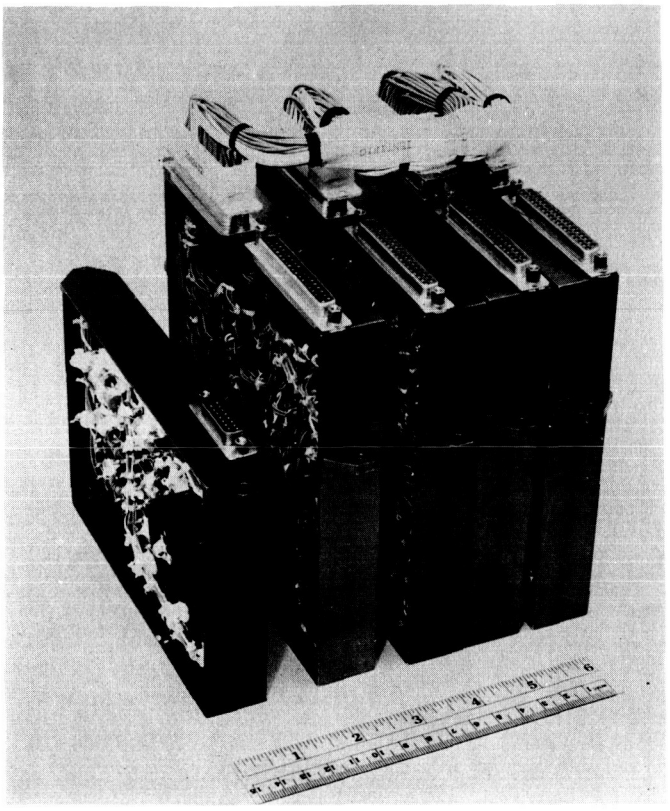

Fig. 2. DAS assembly

2. Pre-Life-Test History of DAS Units

Two *Mariner II* DAS units were selected for life testing: a proof test model (the first unit delivered by the contractor) and a flight spare (the last unit delivered by the contractor).

a. Proof test model. Upon delivery of the system, electrical tests were run to determine correct operation, with modifications and repairs made where necessary. After the system was qualified electrically, the unit was delivered to the spacecraft complex to be used to check both electrical and mechanical interfaces with the scientific instruments and the spacecraft.

Because of a conflict between the proof-test-model testing, the flight-acceptance testing of the first flight DAS, and the spacecraft schedule, the proof-test-model DAS was not subjected to flight environment testing. However, the unit was temperature-tested in the DAS laboratory both before and during the life test.

No component testing or quality assurance measures were imposed on its fabrication as were imposed on that of the flight units. The quality of the unit was not completely acceptable to JPL quality-control personnel.

b. Flight spare. Since this unit was a flight spare, flight-acceptance tests were required. The system was delivered to the spacecraft after the first acceptance testing was completed. Quality-control inspection revealed connector pin retention to be out-of-specification to such a degree that all connectors had to be replaced. Replacement of the connectors and wiring harness was of such major significance to the reliability of the over-all system that a rerun of the complete series of flight-acceptance tests was necessary. On completion of these tests, the system was returned to the spacecraft and accepted as a flight spare.

3. DAS Life Tests

a. Proof test model. The accumulated operating time on the system before the start of the life test was 284 hr. Approximately 100 hr of this operating time was spent on the spacecraft.

The objective of the life test was to run the unit continuously and periodically check the voltage margins. This was done by varying the supply voltages (12, 6, and −6 v), one at a time, to obtain what is called a "shmoo diagram" (Fig. 3)[1]. During each subsequent margin check, any variations in the margins were observed as functions of time. A relay rack (Fig. 4) with the necessary equipment to simulate input signals and output loading comprised the life-test setup. The test was run at room temperature, except for an 8-hr sterilization heat soak at 125°C and a 2-wk period when the temperature was elevated to 150°F.

The life test was begun on March 21, 1962, with voltage margin information compiled in the DAS log. During the first part of the test (approximately 400 hr), a number of logic and circuit modifications were made to the DAS (modified to flight configuration) and to the test gear. No effort was made to qualify parts or ensure quality in workmanship; thus, in two cases after a modification was made, the DAS did not operate properly when power was applied. In each case, when the problem was found and repaired, normal operation was restored. These two cases were not considered a system failure during the life test.

On April 26 (716 hr on the hour meter), margins were checked. The shmoo diagram was generated at this time. Voltage margins had not changed after 716 hr of life test-

[1]Wolfe, J. L., *Progress Report, Mariner "R" Data Conditioning System Life Test,* Interoffice Memorandum, Jet Propulsion Laboratory, Pasadena, California, August 20, 1962.

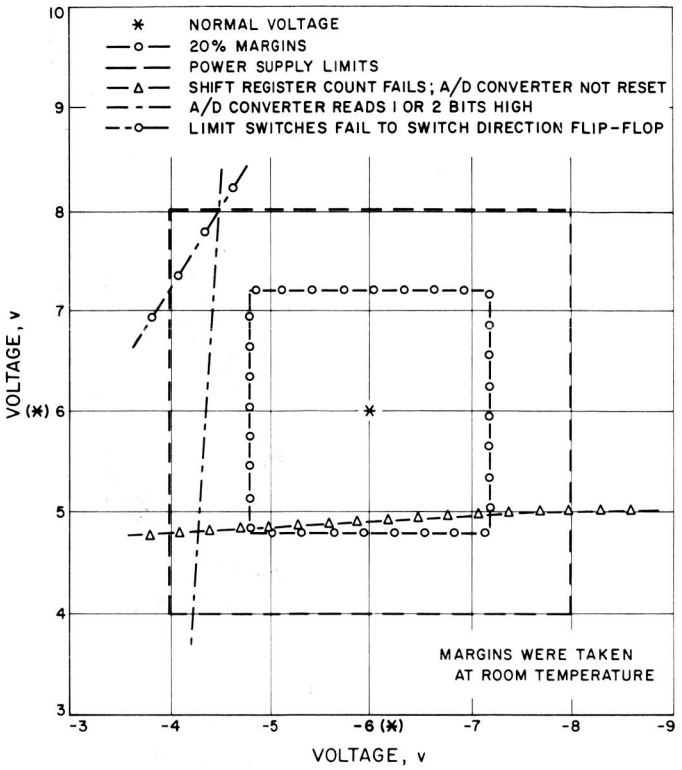

Fig. 3. Shmoo diagram obtained during proof-test-model DAS life test

ing. At 857 hr of operation, the DAS was subjected to a sterilization temperature of 125°C for 8 hr. Operational checks were made periodically to determine proper operation of the system. Completed margin checks were made at 876, 2438, and 3810 hr. No change in margins was detected up to and including 3810 hr of operation.

On October 15, the system was placed in the temperature chamber to begin a 2-wk test at elevated temperatures. The test was run to simulate the thermal environment the *Mariner II* spacecraft was expected to encounter during the mission. The starting temperature was 115°F. After 18 hr at this temperature, a failure was noted in system operation. The failure was traced to an emitter–follower module. An analysis of the module by the contractor indicated a bad solder joint caused by the clipping of a transistor lead after the soldering operation. A thorough inspection of the module would have located the bad solder joint. The total life-test operating time up to the time of the failure was 4478 hr. The emitter–follower module was replaced, and the 2-wk temperature test continued. The temperature was increased to 150°F and left at that point for the last 7 days of the test. No other failure occurred. A margin check at 4852 hr showed no change in the operating margins.

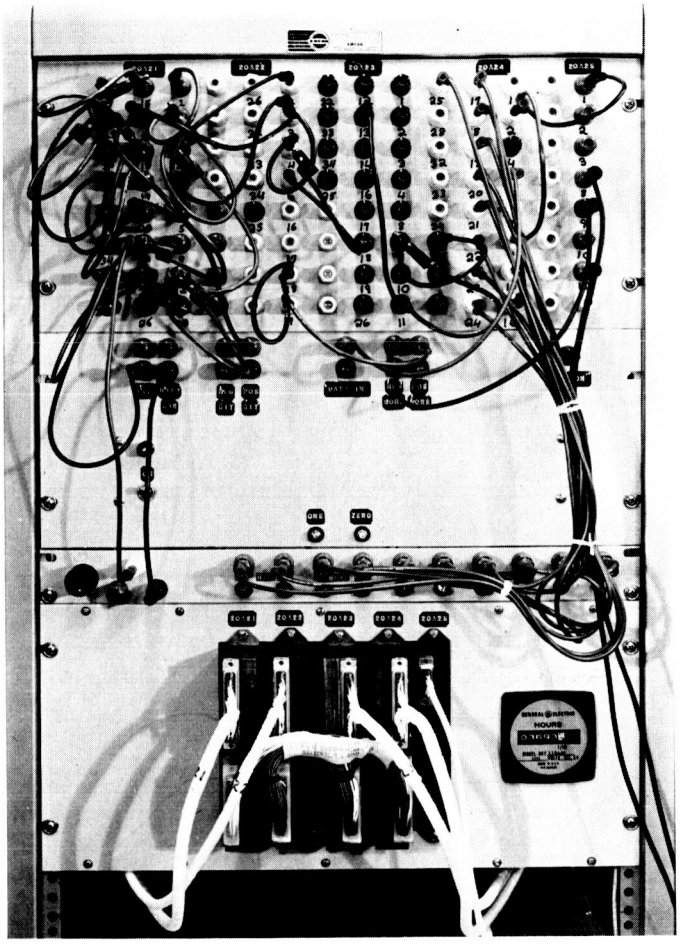

Fig. 4. DAS life-test setup

On February 13, 1963, after accidental shorting of the output stages, the test was stopped and the proof-test-model DAS was removed. The system had run for 7016 hr with one failure.

b. Flight spare. After launch of the two *Mariner* Venus 1962 spacecrafts (*Mariners I* and *II*), the flight spare DAS was returned to JPL. Accumulated operating time before start of the life test was 118 hr. The system was installed in the life-test rack, and the test was begun on May 28, 1963 (hour meter reset to zero). Margin tests to generate a shmoo diagram were not run. However, checks on proper operation were run as time permitted.

The latest operational check was conducted on February 2, 1965. Data printed out and the event monitoring system indicated all functions are normal. The elapsed hour meter reading on February 3, 1965, was 12,960 hr. The test will continue until a failure occurs or a decision is made to stop the test.